



Article

Genome-Wide Identification and Characterization of *DnaJ* Gene Family in Grape (*Vitis vinifera* L.)

Tianchi Chen ¹, Tao Xu ¹, Tianye Zhang ² , Tingting Liu ², Leyi Shen ¹, Zhihui Chen ³, Yueyan Wu ^{1,*} and Jian Yang ^{2,*}

¹ College of Biological and Environmental Sciences, Zhejiang Wanli University, Ningbo 315100, China; tianchichen1997@163.com (T.C.); xu562891@163.com (T.X.); strugture@126.com (L.S.)

² State Key Laboratory for Quality and Safety of Agro-Products, Institute of Plant Virology, Ningbo University, Ningbo 315211, China; ZTye1995@163.com (T.Z.); anatk6@163.com (T.L.)

³ School of Life Sciences, University of Dundee, Dundee DD1 5EH, UK; z.y.chen@dundee.ac.uk

* Correspondence: wyynb2009@163.com (Y.W.); nather2008@163.com (J.Y.); Tel.: +86-574-8822-2235 (Y.W.)

Abstract: Grape production in southern China suffers great loss due to various environmental stresses. To understand the mechanism of how the grape plants respond to these stresses is an active area of research in developing cultivation techniques. Plant stress resistance is known to rely on special proteins. Amongst them, DnaJ protein (HSP40) serves as co-chaperones of HSP70, playing crucial roles in various stress response. However, the DnaJ proteins encoded by the *DnaJ* gene family in *Vitis vinifera* L. have not been fully described yet. In this study, we identified 78 *VvDnaJs* in the grape genome that can be classified into three groups—namely, DJA, DJB, and DJC. To reveal the evolutionary and stress response mechanisms for the *VvDnaJ* gene family, their evolutionary and expression patterns were analyzed using the bioinformatic approach and qRT-PCR. We found that the members in the same group exhibited a similar gene structure and protein domain organization. Gene duplication analysis demonstrated that segmental and tandem duplication may not be the dominant pathway of gene expansion in the *VvDnaJ* gene family. Codon usage pattern analysis showed that the codon usage pattern of *VvDnaJs* differs obviously from the monocotyledon counterparts. Tissue-specific analysis revealed that 12 *VvDnaJs* present a distinct expression profile, implying their distinct roles in various tissues. *Cis*-acting element analysis showed that almost all *VvDnaJs* contained the elements responsive to either hormones or stresses. Therefore, the expression levels of *VvDnaJs* subjected to exogenous hormone applications and stress treatments were determined, and we found that *VvDnaJs* were sensitive to hormone treatments and shade, salt, and heat stresses, especially VIT_00s0324g00040. The findings of this study could provide comprehensive information for the further investigation on the genetics and protein functions of the *DnaJ* gene family in grape.

Keywords: grape; the *DnaJ* gene family; phytohormone; abiotic stress



Citation: Chen, T.; Xu, T.; Zhang, T.; Liu, T.; Shen, L.; Chen, Z.; Wu, Y.; Yang, J. Genome-Wide Identification and Characterization of *DnaJ* Gene Family in Grape (*Vitis vinifera* L.).

Horticulturae **2021**, *7*, 589.

<https://doi.org/10.3390/horticulturae7120589>

<https://doi.org/10.3390/horticulturae7120589>

Academic Editor: Lijun Wang

Received: 9 November 2021

Accepted: 15 December 2021

Published: 18 December 2021

Publisher's Note: MDPI stays neutral with regard to jurisdictional claims in published maps and institutional affiliations.



Copyright: © 2021 by the authors. Licensee MDPI, Basel, Switzerland. This article is an open access article distributed under the terms and conditions of the Creative Commons Attribution (CC BY) license (<https://creativecommons.org/licenses/by/4.0/>).

1. Introduction

Grape (*Vitis vinifera* L.), as a non-climacteric and economical fruit, has been world widely cultivated [1,2]. Grape production is often limited by various abiotic and biotic stresses during growth and development, especially the heat wave in summer. According to the recent evaluation on the global climate, the global surface average temperature has reached 16.73 °C, the highest during the last 142 years. Increasing air temperature exacerbates the detrimental impact on grape growth and development and drastically influences the yield of grape production. In addition to heat stress, shade stress is also a common environmental limitations during grape cultivation, which causes lower air flow and directly alters soil temperature and humidity [3]. Salt stress is one of the most detrimental environmental stresses as well, which leads to a series of responses at the morph-physiological and molecular levels with increasing exposure of soil salinity due to salt-induced ionic toxicity, osmotic, and ionic stress [4]. It was reported that 20% of

irrigated soils are suffering from salt stress globally [5]. For instance, the sea reclamation often occurs in Ningbo, Zhejiang area on the Chinese middle east coastline, which causes the salinization of soil and consequently the damage on grape growth and fruit yield.

In response to the stresses mentioned above, the heat shock protein (HSP) system is believed to be involved and play key roles. As a highly conserved family of molecules, HSPs are involved in protein folding, assembly, translocation, and degradation [6,7]. HSPs belong a large class of protein, normally classified into six types—including HSP100, HSP90, HSP70, HSP60, HSP40 and other small heat shock protein families—based on their molecular weights [8]. HSP40—also known as the DnaJ protein—is a family of protein chaperones which functions either alone or in combination with their partner Hsp70s and stimulates the ATP hydrolysis activity of HSP70s [9,10]. The enhanced ATP hydrolysis activity of HSP70 is essential for the stable binding and proper folding of its interaction proteins [11]. These are the key components contributing to cellular protein homeostasis under various biotic and abiotic stresses [12].

DnaJ proteins can be classified into three categories (Type-A, Type-B and Type-C) based on the type and combination of the conserved domains. The conserved domains include J-domain, Gly/Phe-rich domain (G/F), CXXCXGXG zinc-finger domain, and C-terminal domain. The J-domain is usually located in the N-terminal, and has a highly conserved HPD tripeptide (His, Pro, and Asp) [13]. The G/F domain is a glycine/phenylalanine-rich flexible region, and may influence the specific partners of DnaJ protein [10]. The C-terminal domain is relatively less conserved and can facilitate DnaJ protein dimerization and also participates in interactions with its substrates [14]. Type-A contains the above four domains. Type-B lacks a zinc-finger domain compared to Type-A. Type-C presents only the J-domain [15]. In addition, the DnaJ-like proteins can be defined as Type-D DnaJ proteins, which are strikingly similar to DnaJ proteins in sequence and structure but lack the HPD motif [16].

At present, a large amount of attention has been directed towards the functions of DnaJ proteins in the biochemical and physiological processes in plants. Previous studies have revealed that chloroplast-targeted DnaJ proteins in tomato can facilitate heat tolerance, reduce the accumulation of reactive oxygen species (ROS), and maintain Rubisco activity under heat stress [9,17]. BIL2, as a member of the DnaJ protein family, can promote plant growth and induce cell elongation to resist against environmental stresses mediated by brassinosteroid signaling through the promotion of ATP synthesis in mitochondria [18]. Overexpression of *GmDnaJ.1* in soybean has caused hypersensitive response (HR) such as cell death and thus this protein may be involved in mRNA splicing and miRNA processing [15]. Meanwhile, silencing *GmDnaJ.1* was able to significantly enhance the susceptibility of soybean plants to mosaic virus, which confirmed its positive defense effect against the virus. DnaJ proteins were further proven to play an important role in virus–plant interactions. For example, the CP of potato virus Y can interact with the DnaJ protein to regulate cell–cell movement during infection [19]. In addition, DnaJ proteins can provide resilience in mitochondrial import processes [20]. In hormone regulation, several studies have found that salicylic acid (SA) can initiate the activation of the expression of *LeCDJ2*, and *AtJ1* may function as a negative regulator of abscisic acid (ABA) response [12,21]. In conclusion, the above studies showed that DnaJ proteins have various biological functions and involved indeed in various abiotic and biotic stresses.

However, the *DnaJ* gene family in *Vitis vinifera* L. has not been systematically analyzed yet. We believe that it is of significance to study DnaJ proteins in grape since the DnaJ proteins has many roles in physiological processes and in response to stresses. In this study, a genome-wide analysis was performed, and 78 candidate genes were identified in the *VvDnaJ* gene family. Then the chromosomal localization, phylogenetic tree, gene structure, conserved motif, protein tertiary structure, multiple sequence comparison, collinearity, codon usage pattern, and *cis*-acting elements of these *VvDnaJ* genes were analyzed using a range of bioinformatics approaches. We have also constructed six GFP-fluorescent vectors to validate subcellular localization predictions of the prior bioinformatics. In addition,

the expression patterns of *VvDnaJs* in different tissues were determined by qRT-PCR. To explore the regulatory mechanisms of the *VvDnaJ* gene family under various hormones and stresses, the expression levels of *VvDnaJs* were determined when the grapes were under hormone, shade, salt, and heat stress conditions. We hope that the results can help illustrate the potential functions of *VvDnaJs* and utilize candidate genes for improving grape stress tolerance.

2. Results

2.1. Identification and Analysis of *VvDnaJs*

The grape genome was firstly screened for DnaJ proteins by using the hidden Markov model (HMM) profiles of DnaJ conserved domain (PF00226), DnaJ central domain (PF00648) and DnaJ C terminal domain (PF01556) in Pfam database. Then, we used the known *DnaJ* sequences in Arabidopsis and rice to blast against the grape genome by the BLASTp search to obtain the grape homologs. All candidate genes obtained were further screened by Pfam, NCBI-CDD, and SMART database, the genes without functional domain (J-domain) were eliminated. Ultimately, a total of 78 *VvDnaJs* were identified in grape genome. The gene ID, CDS length, protein size, and the prediction of theoretical pI, molecular weight, subcellular localization, and signal peptides are shown in Table 1. The size of the *VvDnaJ* protein varied from 72 (VIT_07s0005g02760) to 2609 (VIT_11s0016g04420) amino acids. The average theoretical pI and molecular weight for *VvDnaJ* proteins were 7.81 and 49.7 kDa, respectively. A secretory signal peptide was present in seven *VvDnaJ* proteins. DnaJ proteins can recruit their HSP70s partner to specific subcellular localization for highly specialized chaperone functions [22]. Fifty-four *VvDnaJ* proteins were predicted to be subcellularly localized in extracellular matrix, followed by nine on plasma membrane and eight in cytoplasm (Table 1). To verify the accuracy of the prediction results, six *VvDnaJ* proteins came from cytoplasm, plasma membrane, and chloroplast were selected for subcellular localization analysis in *N. benthamiana* leaves. GFP fluorescence for VIT_06s0080g01230 (predicted to be localized in the cytoplasm) was observed in the cytoplasm and VIT_01s0026g01450 (predicted to be localized in the cytoplasm) was observed in the cytoplasm and nuclear. The subcellular localization result of VIT_01s0026g01450 does not perfectly fit to the predicted results. Previous studied reported that some HSP70s was located in nuclear [23]. DnaJ protein serves as cochaperones of HSP70, suggesting that VIT_01s0026g01450 may interact with HSP70 and exert its function in nuclear. However, it is also possible that the difference in subcellular localization result was due to species differences between grape and *Nicotiana tabacum* L. GFP fluorescence for VIT_05s0077g02380, VIT_11s0016g05120, and VIT_18s0086g00580 (predicted to be localized in the plasma membrane) was coincided with the plasma membrane marker RFP-TM23, indicating that these *VvDnaJ* proteins were located in the plasma membrane. GFP fluorescence for VIT_00s0362g00010 (predicted to be localized in the chloroplast) was coincided with the chloroplast, indicating that VIT_00s0362g00010 was located in the chloroplast (Figure 1). The above results were consistent with the prediction results. GO analysis showed that about one-third of *VvDnaJ* proteins were involved in the process of protein folding in biological process and protein binding in molecular function. Additionally, half of the *VvDnaJ* proteins were associated with the cytoplasm in the cellular component (Figure 2).

Table 1. Gene ID, CDS length, protein size, and the prediction of theoretical pI, molecular weight, subcellular localization, and signal peptides for each *VvDnaJ*.

Gene Name	Type	Chromosomal Distribution	CDS Length	Protein Size	Theoretical pI	Molecular Weight	Subcellular Localization	Signal Peptides
VIT_01s0011g00790	DJC	Chr1: 710539-714104	1950	649	8.15	74,483	Extracellular	None
VIT_01s0011g03790	DJC	Chr1: 3429615-3441498	1248	415	5.92	45,912	Plasma membrane	None
VIT_01s0011g04820	DJC	Chr1: 4436645-4438196	507	168	6.18	19,610	Extracellular	None
VIT_01s0026g00840	DJC	Chr1: 9697764-9711600	1227	408	8.53	46,044	Plasma membrane	None
VIT_01s0026g01450	DJB	Chr1: 10418267-10420055	822	273	9.52	31,045	Cytoplasmic	None
VIT_01s0010g03760	DJC	Chr1: 21117742-21120902	2454	817	8.59	90,798	Extracellular	None
VIT_01s0010g03770	DJC	Chr1: 21126528-21128523	729	242	9.55	26,551	Extracellular	None
VIT_02s0154g00550	DJC	Chr2: 5296962-5325864	1614	537	8.98	59,496	Plasma membrane	None
VIT_02s0012g02290	DJC	Chr2: 9220337-9222116	1776	591	9.26	68,065	Extracellular	None
VIT_03s0038g02110	DJC	Chr3: 1449330-1451521	456	151	9.68	17,257	Extracellular	None
VIT_03s0038g04420	DJC	Chr3: 3205478-3213940	1011	336	6.64	37,724	Extracellular	None
VIT_03s0088g00390	DJC	Chr3: 8414516-8423780	1026	341	9.29	38,310	Extracellular	None
VIT_03s0017g00300	DJC	Chr3: 14583926-14585707	1461	486	5.15	53,581	Extracellular	None
VIT_04s0008g01770	DJC	Chr4: 1382423-1384601	645	214	6.77	24,104	Extracellular	None
VIT_04s0008g04300	DJB	Chr4: 3680859-3684659	1020	339	8.86	37,058	Cytoplasmic	None
VIT_04s0023g03470	DJC	Chr4: 20028906-20029894	606	201	9.02	22,502	Extracellular	None
VIT_04s0044g00490	DJC	Chr4: 21276992-21300325	858	285	9.77	32,810	Extracellular	None
VIT_05s0077g00580	DJC	Chr5: 388198-396327	2244	747	9.1	82,639	Extracellular	None
VIT_05s0077g02380	DJC	Chr5: 1910184-1911679	1062	353	7.63	41,094	Plasma membrane	None
VIT_05s0020g02050	DJC	Chr5: 3805550-3809148	2508	835	5.34	94,619	Extracellular	None
VIT_05s0020g04120	DJC	Chr5: 5772852-5780510	549	182	4.43	20,345	Extracellular	None
VIT_05s0029g00500	DJC	Chr5: 15301515-15303244	651	216	9.69	24,466	Membrane bound chloroplast	None
VIT_06s0004g05140	DJC	Chr6: 6080876-6084357	849	282	6.06	31,904	Extracellular	Yes
VIT_06s0009g00270	DJC	Chr6: 10340297-10360270	741	246	9.29	29,363	Extracellular	None
VIT_06s0061g00090	DJC	Chr6: 17293997-17317439	3210	1069	5.66	118,065	Extracellular	None
VIT_06s0080g01230	DJA	Chr6: 21412098-21415608	1254	417	5.78	46,358	Cytoplasmic	None
VIT_07s0005g01220	DJB	Chr7: 3750414-3757370	1038	345	5.99	38,873	Endoplasmic reticulum	Yes
VIT_07s0005g02760	DJC	Chr7: 5033390-5035659	219	72	9.99	8036	Extracellular	None
VIT_07s0129g00480	DJC	Chr7: 15715343-15720091	1569	522	6.71	59,464	Extracellular	None
VIT_08s0105g00350	DJB	Chr8: 7542314-7557322	1017	338	9.24	37,358	Cytoplasmic	None
VIT_08s0217g00090	DJC	Chr8: 8204077-8210204	1833	610	9.41	66,957	Extracellular	Yes
VIT_08s0040g00120	DJC	Chr8: 11031671-11038538	519	172	9.57	19,237	Plasma membrane	None
VIT_08s0040g02090	DJC	Chr8: 13199639-13205358	1425	474	5.92	52,783	Extracellular	Yes
VIT_08s0007g06530	DJC	Chr8: 20258210-20262858	786	261	9.13	30,015	Extracellular	None
VIT_08s0007g07380	DJC	Chr8: 20936611-20939266	930	309	9.41	34,898	Extracellular	None
VIT_08s0007g07960	DJC	Chr8: 21361191-21366038	876	291	8.11	33,289	Nuclear	None
VIT_08s0007g09040	DJC	Chr8: 22381356-22383986	1686	561	5.28	64,094	Extracellular	None

Table 1. Cont.

Gene Name	Type	Chromosomal Distribution	CDS Length	Protein Size	Theoretical pI	Molecular Weight	Subcellular Localization	Signal Peptides
VIT_09s0002g00690	DJC	Chr9: 460481-463477	732	243	6.1	26,948	Extracellular	None
VIT_09s0002g07210	DJA	Chr9: 7150525-7184468	1470	489	8.96	52,719	Extracellular	None
VIT_09s0018g00620	DJC	Chr9: 16881863-16882927	459	152	5.25	17,357	Chloroplast	None
VIT_10s0116g00420	DJC	Chr10: 204741-208123	1236	411	9.31	47,334	Plasma membrane	None
VIT_10s0003g00260	DJB	Chr10: 1559664-1561563	1029	342	9.12	37,846	Cytoplasmic	None
VIT_10s0042g00960	DJC	Chr10: 14458409-14461750	1497	498	9.22	54,930	Extracellular	None
VIT_11s0016g04420	DJC	Chr11: 3708675-3733206	7830	2,609	5.84	284,387	Extracellular	None
VIT_11s0016g05120	DJC	Chr11: 4399836-4403087	1074	357	8.13	40,166	Plasma membrane	None
VIT_12s0028g01740	DJC	Chr12: 2373445-2379438	996	331	8.43	37,242	Extracellular	None
VIT_12s0057g00710	DJC	Chr12: 9329408-9331895	2085	694	7.85	76,528	Extracellular	None
VIT_13s0073g00560	DJA	Chr13: 14441307-14444078	1251	416	6.11	46,240	Cytoplasmic	None
VIT_13s0064g01360	DJA	Chr13: 23242305-23254584	1356	451	8.93	49,119	Mitochondrial	None
VIT_14s0060g01490	DJC	Chr14: 1175091-1176374	486	161	5.05	17,980	Extracellular	None
VIT_14s0128g00490	DJC	Chr14: 3110690-3113953	798	265	5.44	29,331	Extracellular	None
VIT_14s0030g00640	DJC	Chr14: 4739769-4743418	3510	1169	8.23	131,034	Extracellular	None
VIT_14s0068g01140	DJC	Chr14: 24933132-24935740	2259	752	5.78	85,287	Extracellular	None
VIT_15s0021g02090	DJA	Chr15: 12895594-12909716	1332	443	6.42	49,332	Cytoplasmic	None
VIT_16s0039g01520	DJC	Chr16: 1113429-1118305	372	123	6.19	14,482	Plasma membrane	None
VIT_16s0050g01460	DJC	Chr16: 18328905-18336293	2067	688	5.72	76,840	Extracellular	Yes
VIT_16s0050g02590	DJC	Chr16: 19570187-19573227	2232	743	9	82,581	Extracellular	None
VIT_17s0000g01150	DJC	Chr17: 818277-821660	2661	886	8.99	97,930	Extracellular	None
VIT_17s0000g02030	DJA	Chr17: 1644223-1656845	1446	481	9.08	53,139	Extracellular	None
VIT_17s0000g05530	DJB	Chr17: 6022005-6029405	1050	349	8.8	39,030	Cytoplasmic	None
VIT_18s0122g00050	DJC	Chr18: 70299-86511	1125	374	5.45	41,925	Extracellular	None
VIT_18s0001g04440	DJC	Chr18: 3852065-3861217	819	272	9.63	32,183	Extracellular	Yes
VIT_18s0001g06970	DJA	Chr18: 5184425-5218375	1044	347	8.54	38,433	Mitochondrial	Yes
VIT_18s0001g07260	DJC	Chr18: 5484997-5490030	417	138	4.71	16,458	Extracellular	None
VIT_18s0001g07450	DJC	Chr18: 5687109-5688423	957	318	8.8	34,752	Extracellular	None
VIT_18s0001g08540	DJC	Chr18: 6978788-6992668	750	249	9.28	29,677	Extracellular	None
VIT_18s0001g14440	DJC	Chr18: 12432955-12439459	660	219	10	24,129	Extracellular	None
VIT_18s0001g15020	DJC	Chr18: 13043063-13050564	1218	405	5.88	45,726	Extracellular	None
VIT_18s0086g00580	DJC	Chr18: 17892148-17892855	486	161	8.34	17,904	Plasma membrane	None
VIT_18s0072g01080	DJC	Chr18: 20620084-20633488	1716	571	8.86	64,865	Extracellular	None

Table 1. Cont.

Gene Name	Type	Chromosomal Distribution	CDS Length	Protein Size	Theoretical pI	Molecular Weight	Subcellular Localization	Signal Peptides
VIT_18s0117g00260	DJC	Chr18: 23472866-23476496	762	253	5.42	28,812	Extracellular	None
VIT_19s0177g00270	DJC	Chr19: 6120151-6131282	855	284	9.24	32,355	Extracellular	None
VIT_19s0177g00280	DJC	Chr19: 6133013-6134771	909	302	8.85	34,404	Extracellular	None
VIT_19s0015g01370	DJC	Chr19: 9657864-9658472	447	148	9.35	16,343	Extracellular	None
VIT_19s0027g00440	DJC	Chr19: 19247402-19265051	1662	553	8.75	63,182	Extracellular	None
VIT_00s0252g00060	DJC	Chr19: 17649954-17669572	4677	1558	6.23	169,621	Extracellular	None
VIT_00s0324g00040	DJA	Chr19: 23409521-23422273	1446	481	9.32	52,150	Extracellular	None
VIT_00s0362g00010	DJC	Chr19: 25688160-25690181	627	208	9.35	23,579	Chloroplast	None

2.2. Phylogenetic and Domain Organization Analysis of *VvDnaJs*

To comprehensively analyze the phylogenetic relationship of the *VvDnaJ* gene family, the phylogenetic tree for grape, rice, and *Arabidopsis thaliana* was constructed using the neighbor-joining method, and their locus IDs and sequences are shown in Table S1. The phylogenetic tree showed that 310 *DnaJs* were classified into three groups and correspondingly named DJA, DJB, and DJC based on previous studies (Figure 3). The number of *DnaJ* genes in the DJA and DJB groups in grape, rice, and *Arabidopsis thaliana* were roughly similar. The number of genes in DJA and DJB groups were significantly less than those of the DJC group in all three species, and the *DnaJ* gene family was predominantly formed by the DJC group (Figure S1).

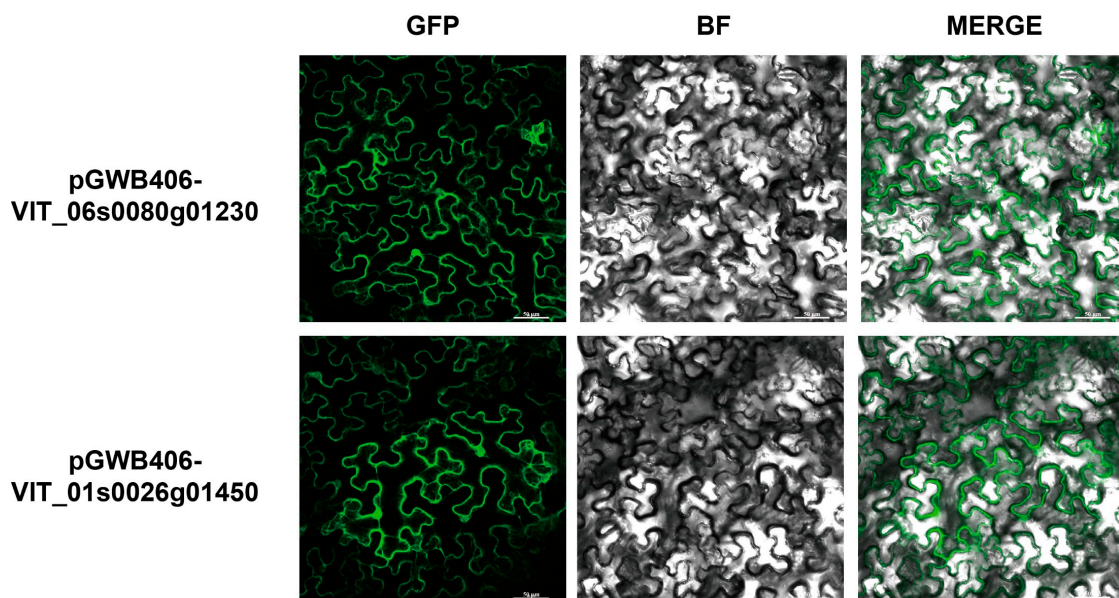


Figure 1. Cont.

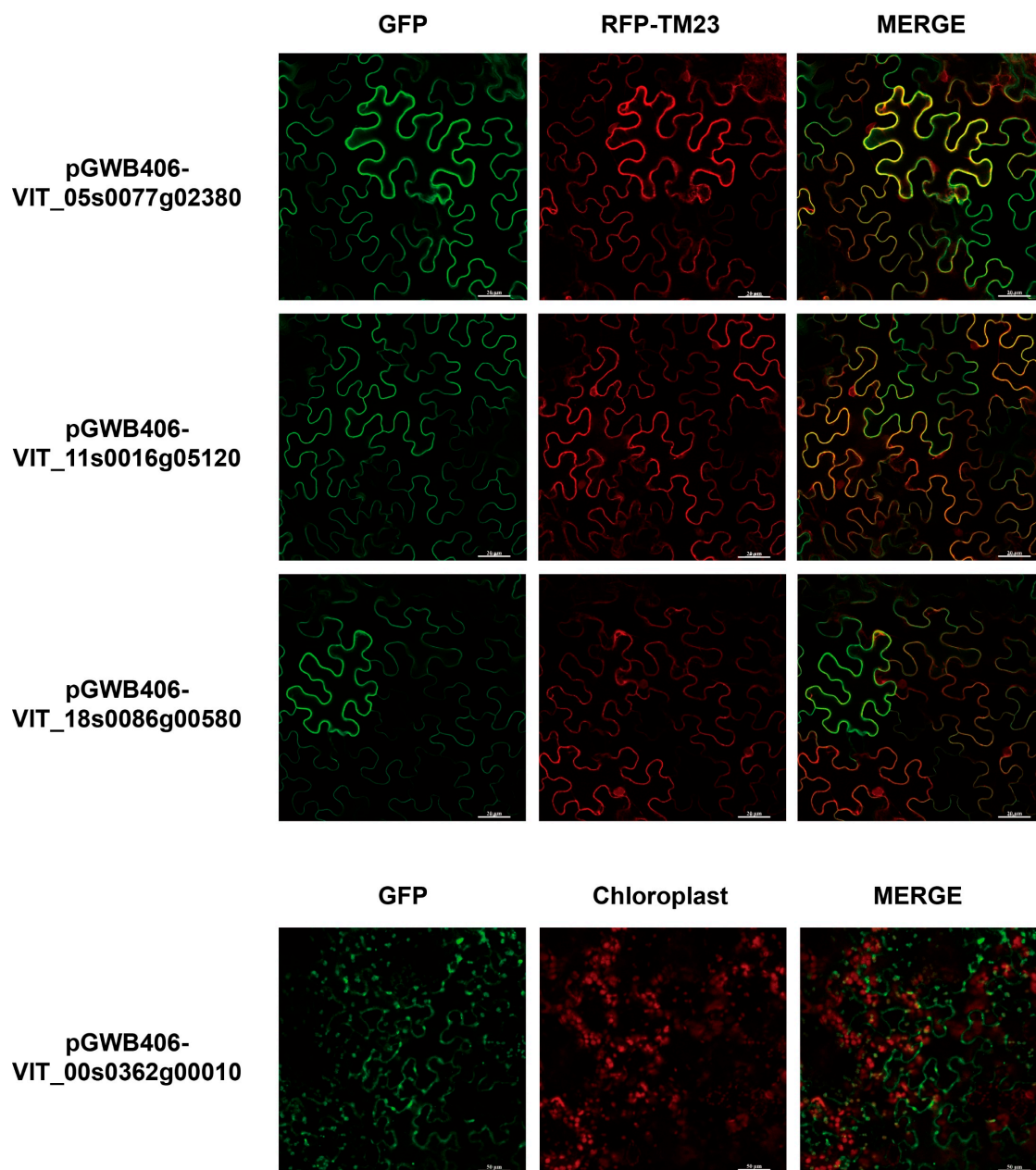


Figure 1. Subcellular localization of six VvDnaJ protein. BF represents bright field. RFP-TM23 is the plasma membrane marker protein.

The three domains in the grape DnaJ protein are the J-domain, zinc-finger domain, and C-terminal domain. A total of 78 VvDnaJ proteins were classified into three types: DJA (8 members), DJB (6 members), and DJC (64 members) (Figure 4). The members of DJA contained all three domains, and C-terminal domains located within the zinc-finger. The members of DJB contained the J-domain and C-terminal domain. The members of DJC contained only the J-domain and were divided into seven clusters according to the domains other than J-domain. The members of Cluster I contained a J-domain at the C-terminus and a DUF3444 domain at the N-terminus. Cluster II contained a DnaJ-X domain at the N-terminus. Members of Cluster III contained Fer4 domains at the midstream of the VvDnaJ proteins. Cluster IV contained a DUF1977 at the N-terminus and J-domain was located at the midstream of VvDnaJ protein. Cluster V contained a Jiv90 domain was located at the N-terminus and followed by the J-domain. Jiv90 in the VvDnaJ protein can interact with viral protein (Jiv) in pestivirus viral polypeptide [24]. The members of Cluster VI were relatively unique, each member was different, so we classified them into one category,

which contained Sec63, Zf, Myb, DUF, RRM, HSCB, TPR, and GYF domains (Figure 4). The TPR domain is a widespread protein domain in all organisms, and plays important roles in protein–protein interactions [24]. The members of Cluster VII presented only a J-domain. All VvDnaJ proteins had a conserved J-domain, which is crucial for VvDnaJ proteins to modulate the activity of their HSP70 partners.

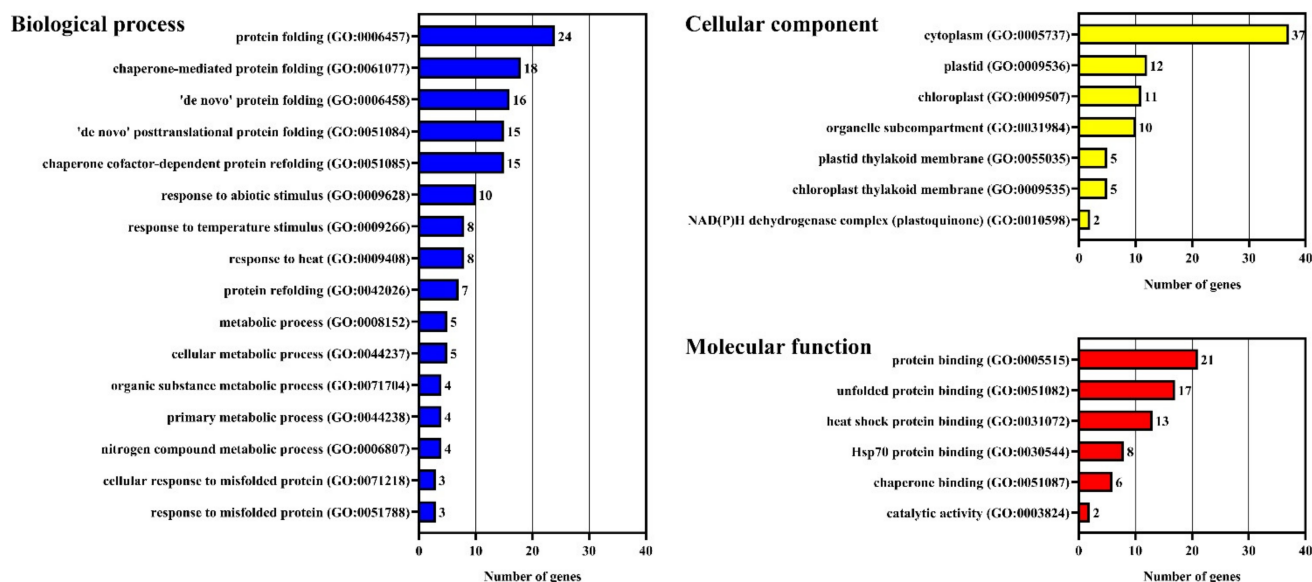


Figure 2. Gene ontology analysis of *VvDnaJ* gene family in three aspects: biological process, cellular component, and molecular function.

2.3. Analysis of Conserved Motif, Gene Structure, Protein Tertiary Structure, and Multiple Sequence Comparison in *VvDnaJs*

The MEME software was used to analyze the conserved motifs of *VvDnaJ* proteins. Nine conserved motifs were found and varied from 15 to 70aa in length among the 78 *VvDnaJ* proteins (Figure S2 and Table S2). The distribution of these motifs in *VvDnaJ* proteins is illustrated in Figure 5a. Each *VvDnaJ* protein contained different numbers of motifs, varying from 1 to 8, and none of the *VvDnaJs* contained all nine motifs. Almost all *VvDnaJ* proteins contained motifs 1–3. The DJA and DJB only contained motifs 1–4, and only the Cluster I of DJC contained motifs 5, 6, 8, and 9. It is noteworthy that the members in the same group exhibited similar motif distribution patterns, which further supported the validity of the group classification result. For example, all the members of the DJB group contained motifs 1–4, and the distribution of the motifs was also similar, motifs 1–3 were located in the C-terminus, and motif 4 was located in the N-terminus. Additionally, we found that motifs 5, 8, and 9 appeared multiple times in Cluster I of DJC. To better understand the structure features of *VvDnaJs*, the exon/intron structures were analyzed using GSDS and are listed in Figure 5b. The number of exons ranged from 1 to 22 among the *VvDnaJs*, and most *VvDnaJs* had more than five exons. The number of exons in Cluster I of DJC was relatively lower compared with the other groups, indicating that these gene structures are more conserved than other groups. Additionally, a total of seven *VvDnaJs* did not exist intron structure. To more intuitive comprehend the structure of *VvDnaJ* proteins, the protein tertiary structures of one or two *VvDnaJ* proteins from each group were selected randomly and predicted using homology-modelling with SWISS-MODEL, and the results are depicted in Figure 5c. The tertiary structures of VIT_00s0324g00040 and VIT_15s0021g02090 were similar, the same was repeated for VIT_08s0105g00350 and VIT_17s0000g05530. We propose that they may have a similar function in the physiological process of the plants. However, the tertiary structures of DJC were more diverse than those of the other groups.

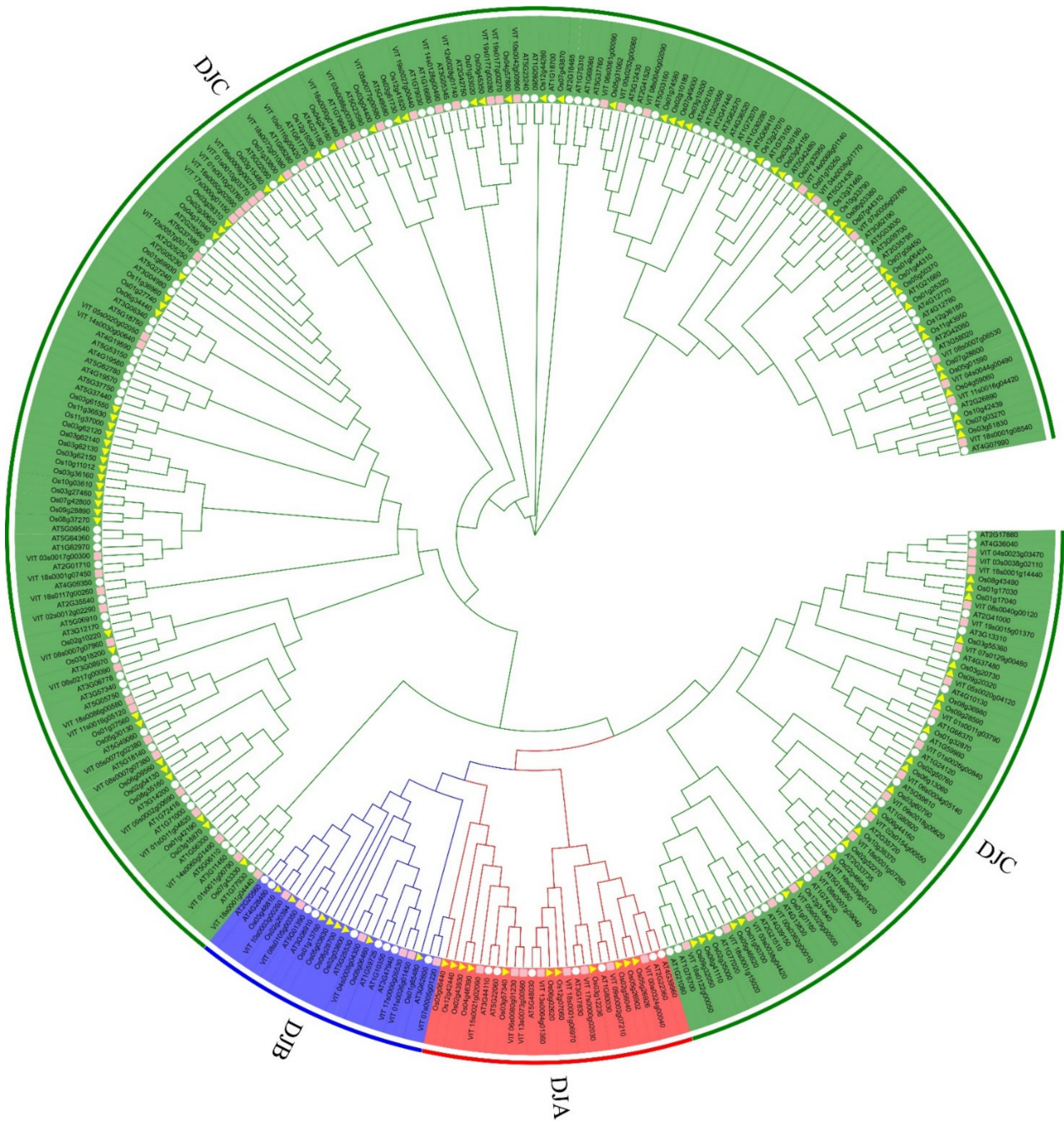


Figure 3. Phylogenetic analysis of *DnaJ* gene family in grape, rice, and *Arabidopsis thaliana*. The pep sequences of 78 *VvDnaJs*, 115 *OsDnaJs*, and 117 *AtDnaJs* were aligned using ClustalW, and the neighbor-joining method was used to construct the phylogenetic tree with the following settings: bootstrap method for phylogeny test; bootstrap replication was set to 1000; p-distance method for substitution model. The DJA, DJB, and DJC groups are indicated by red, blue, and green, respectively, in peripheral circle and inner circle branches. Rectangle, triangle, and circle indicate grape, rice, and *Arabidopsis thaliana*, respectively.

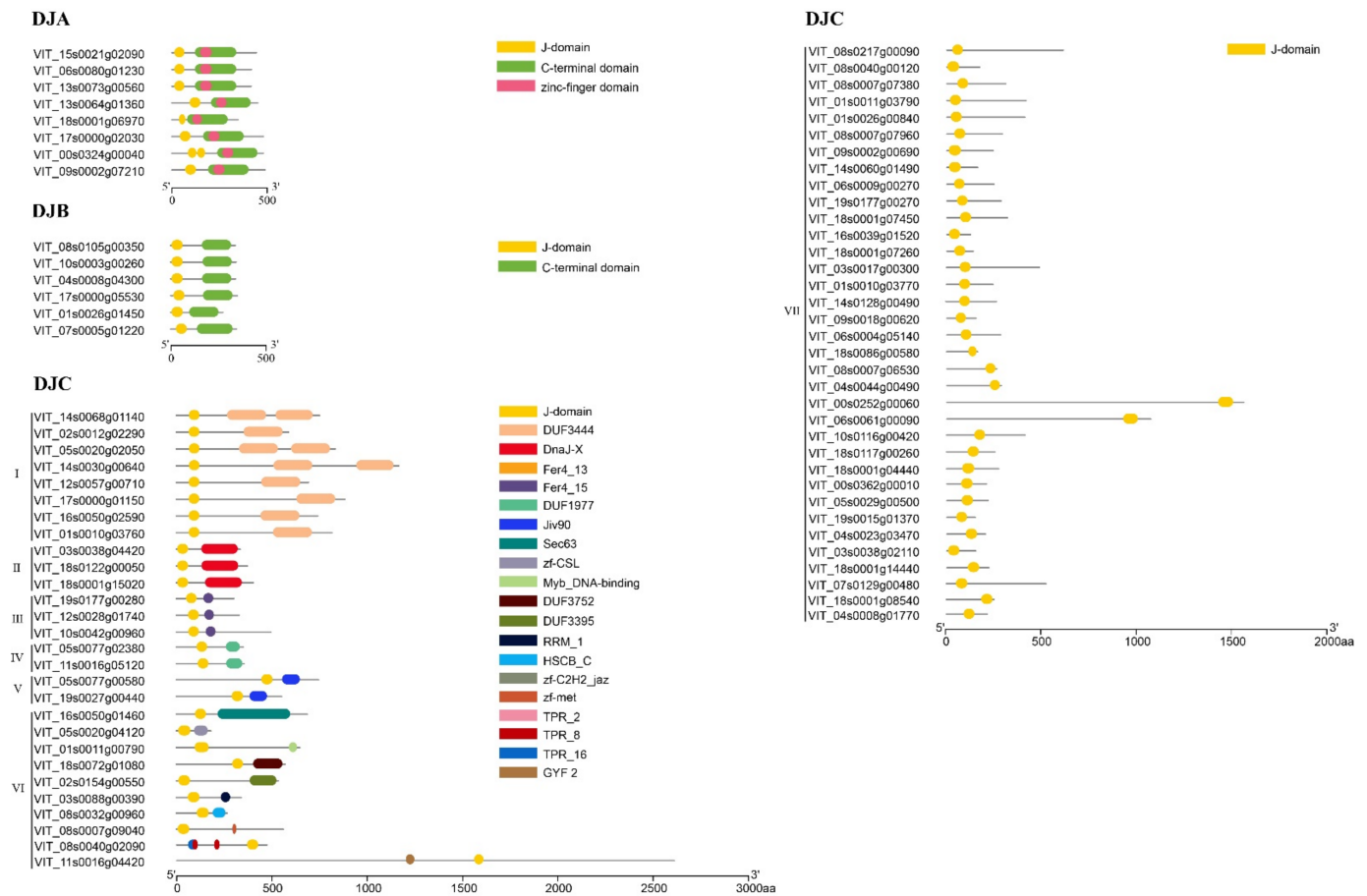


Figure 4. Domain architecture analysis of *VvDnaJ* gene family. The members of *VvDnaJ* gene family were classified into three types (DJA, DJB, and DJC). Clusters I–VII represent the seven different domain combinations in DJC group.

To present the relationship between conserved motifs and domains more intuitively, the multiple sequence comparison in DJA and DJB groups was performed using ClustalW programs. We discovered that the J-domain was composed of motif 3, 1, and 2, and motif 4 was located in the C-terminal domain, suggesting that motifs 1–4 played a critical role in the function of domains. In addition, a well conserved HPD tripeptide was observed in the J-domain (Figure S3), which is a vital criterion for identifying the *DnaJ* gene family. The HPD tripeptide is essential for its ability to accelerate the ATPase activity of Hsp70 [25]. The above results may have shed some insights for further evolutionary analysis and subsequent functional research on *DnaJ* proteins.

2.4. Chromosomal Distribution and Gene Duplication Analysis of *VvDnaJs*

The chromosomal distributions of each *VvDnaJ* are shown in Figure S4. The *VvDnaJs* were randomly distributed across 20 chromosomes. Eleven (14.1%) *VvDnaJs* were mapped to Chr18. There was only one *VvDnaJ* located in Chr15. In addition, the members of the DJC group were distributed on all chromosomes, except for Chr15.

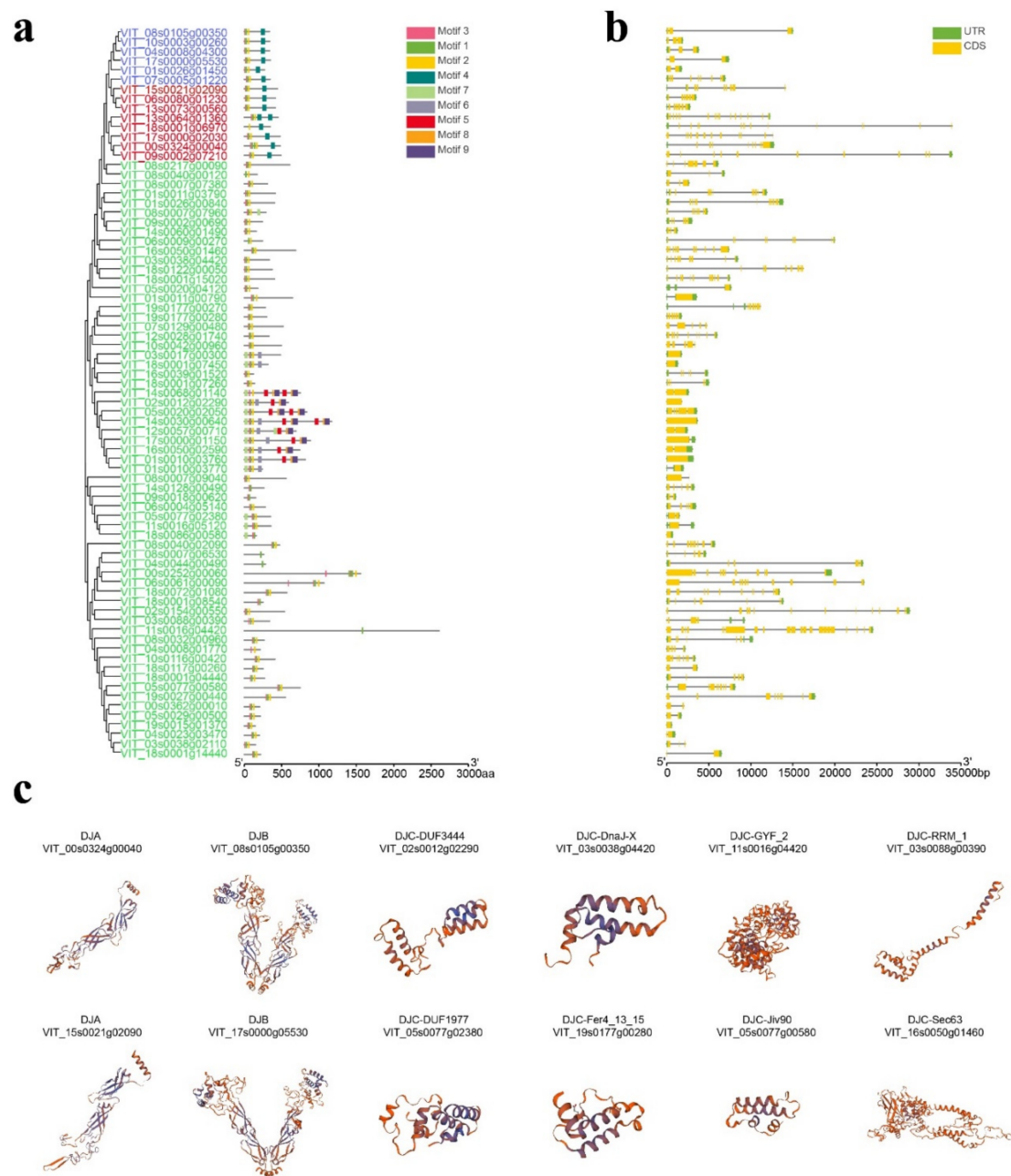


Figure 5. Conserved motif, gene structure, and protein tertiary structure analysis in *VvDnaJ* gene family. **(a)** Motifs 1–9 were performed by MEME and displayed in different colored boxes in each *VvDnaJ* protein. **(b)** Gene structure was determined with the GSDS and displayed in green and yellow boxes. The green boxes represent the UTR sequences, and the yellow boxes represent the coding sequences. **(c)** The protein tertiary structures of 12 *VvDnaJ* proteins were predicted in SWISS-MODEL, and the best results were selected based on QMEAN and GMQE values.

The member of the gene family was derived mostly from the same ancestor, and the ancestor formed the gene family through gene duplication [26]. Gene duplication played a key role in the generation of the gene family, which provided new material to form new genes and promoted the generation of new functions. Six segmental duplications and two tandem duplications were identified using MCScanX in the *VvDnaJ* gene family (Table 2). Six pairs of segmental duplications were observed between Chr17 and Chr1 (VIT_17s0000g05530 and VIT_01s0026g01450), Chr18 and Chr3 (VIT_18s0122g00050 and VIT_03s0038g04420), Chr4 and Chr18 (VIT_04s0023g03470 and VIT_18s0001g14440), Chr3 and Chr18 (VIT_03s0038g02110 and VIT_18s0001g14440), Chr3 and Chr4 (VIT_03s0038g02110 and VIT_04s0023g03470), Ch14

and Chr5 (VIT_14s0030g00640 and VIT_05s0020g02050) (Figure 6). A total of nine *VvDnaJs* with six pairs associated with segmental duplications account for 11.54% (9/78) of all the *VvDnaJs*, and four *VvDnaJs* with two pairs associated with tandem duplications account for 5.13% (4/78). The total duplication ratio of *VvDnaJs* was 16.67%, which is much lower than the grape genome duplication ratio (41.4%), which indicated that the segmental and tandem duplications contributed little to the expansion of the *VvDnaJ* gene family.

Table 2. Calculation of Ka , Ks , and Ka/Ks and divergent time of *VvDnaJ* gene pairs.

Duplicated Gene Pairs	Ka	Ks	Ka/Ks	Duplicated Type	Time (Mya)
VIT_17s0000g05530/VIT_01s0026g01450	0.23	1.23	0.19	Segmental	7.59
VIT_18s0122g00050/VIT_03s0038g04420	0.34	3.25	0.11	Segmental	11.40
VIT_04s0023g03470/VIT_18s0001g14440	0.50	1.70	0.29	Segmental	16.59
VIT_03s0038g02110/VIT_18s0001g14440	0.23	1.57	0.15	Segmental	7.68
VIT_03s0038g02110/VIT_04s0023g03470	0.27	1.19	0.22	Segmental	8.90
VIT_14s0030g00640/VIT_05s0020g02050	0.35	1.32	0.26	Segmental	11.56
VIT_01s0010g03760/VIT_01s0010g03770	0.02	0.05	0.32	Tandem	0.54
VIT_19s0177g00270/VIT_19s0177g00280	0.15	0.24	0.63	Tandem	5.07

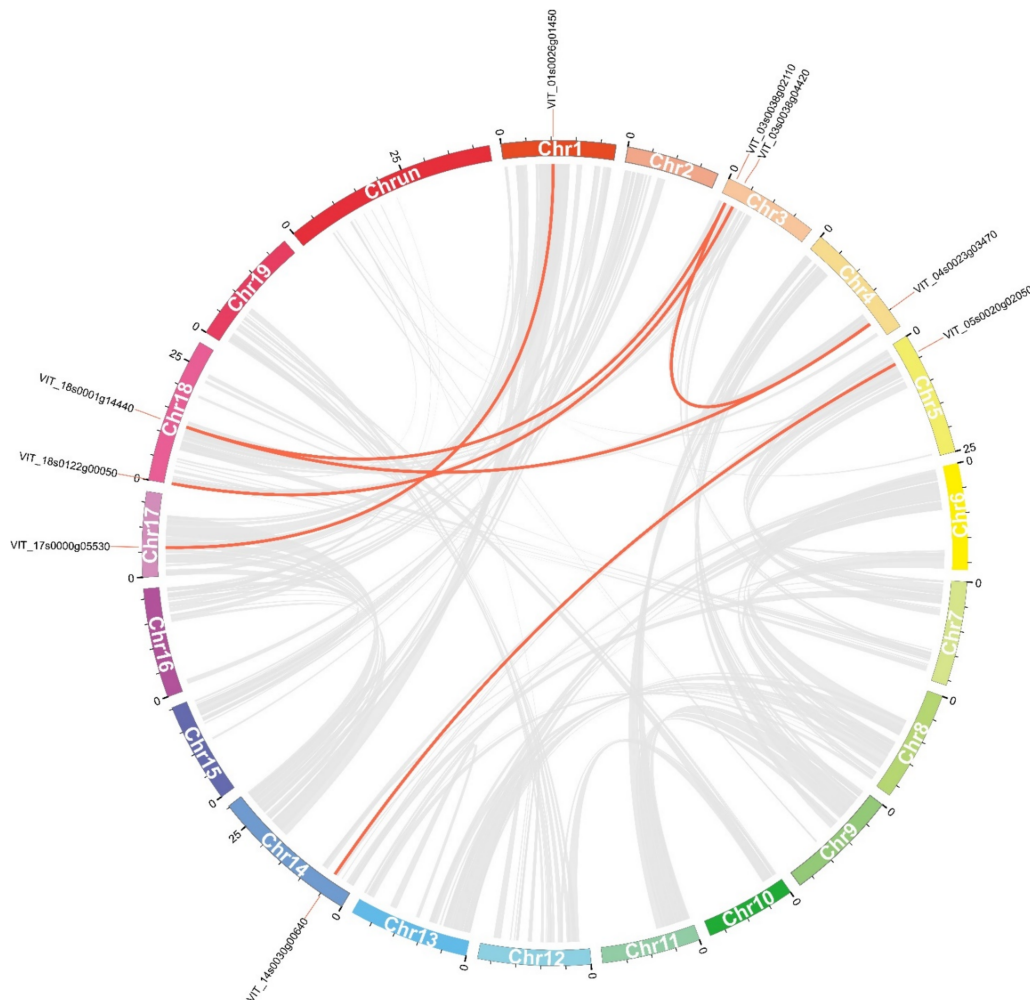


Figure 6. Segmental duplication analysis of *VvDnaJs*. The segmental duplication analysis of *VvDnaJs* was calculated by MCScanX and the results of segmental duplications were displayed by circus. The different colored panels represent different chromosomes, and the chromosome numbers are marked in its panels. Red lines connect homologous genes and represent the duplication events.

To understand the duplication process of *VvDnaJs* over the past several million years, six segmental duplications and two tandem duplications were analyzed using the *KaKs_calculator* to calculate the *Ka* and *Ks* values (Table 2). The results showed that the *Ka/Ks* ratios of eight *VvDnaJ* gene pairs were less than one, which indicated that these genes had undergone purify selection at a low evolutionary rate [27], and this selection would eliminate deleterious mutations in grape. The *Ks* values were used to calculate the divergence time of eight gene pairs, which ranged from 0.54 to 16.59 Mya.

2.5. Analysis of Codon Usage Pattern in *DnaJ* Genes

The pattern of codon usage reveals a fundamental feature of molecular evolution and constitutes an exclusive property for each species and its genome [28,29]. Therefore, we first calculated the codon usage percentage of T3s, G3s, A3s, C3s, GC3s, and GC in six different species (Figure 7a and Table S3). In *Vitis vinifera* L., the usage percentage of C3s and G3s was much lower than that of A3s and T3s, while the opposite behavior was observed in monocotyledon. The usage percentage of GC was significantly higher in monocotyledon, which indicated that the codon preference of monocotyledon was much stronger than *Vitis vinifera* L. and was less likely to be heterologously expressed in *Vitis vinifera* L. In *Vitis vinifera* L., the percentage of G3s/C3s and T3s/A3s was basically equal. The correlation analysis of the nucleotide composition at the third codon position for *Vitis vinifera* L. is shown in Figure 7b. Significant positive relationships were observed among G3s, C3s, GC3s, and GC, indicating that the codon usage pattern of *VvDnaJs* was largely affected by mutation pressure. We further examined the effect of mutation pressure on the degree of variability in synonymous codons by plotting the GC3 values against Effective Number of Codon (ENC) values for each set of genes (Figure 7c and Figure S5). The results showed that the ENC values of almost all *DnaJ* genes in *Vitis vinifera* L., *Capsicum annuum* L., *Brassica oleracea*, and *Arabidopsis thaliana* (dicotyledon) ranged from 40 to 60, showing no obvious codon bias. However, the ENC values of some *DnaJ* genes in *Triticum aestivum* and *Oryza sativa* (monocotyledon) were around 20 to 40, indicating that these genes had a significant codon usage preference. Parity rule 2 (PR2) is considered as an important evaluation index that evaluates whether the bias was mainly induced by mutation pressures, natural selection, or other factors [30]. In the *DnaJ* gene family, most points were located in the bottom right corner (Figure 7d and Figure S5), the T3s was used more frequently than A, and codon G was used more frequently than C. This revealed that the codon usage patterns of *DnaJ* genes have resulted from a combination of mutation pressures and natural selection.

We further performed relative synonymous codon usage (RSCU) analysis to describe the codon usage pattern among different species. By observing the heatmap (Figure 7e and Table S4), most codons were used less frequently than expected in six species ($RSCU \leq 1$). In addition, there were significant differences among species in the RSCU. For example, AGA had a significant preference in dicotyledon ($RSCU > 2$), and it was relatively low in *Triticum aestivum* and *Oryza sativa*. In *Vitis vinifera* L., the *DnaJ* genes exhibited more bias towards A/T-ending codons compared to G/C-ending codons, and this situation was reversed in monocotyledon. The difference between monocotyledon and dicotyledon in the codon usage pattern was likely to be due to mutation pressure and natural selection.

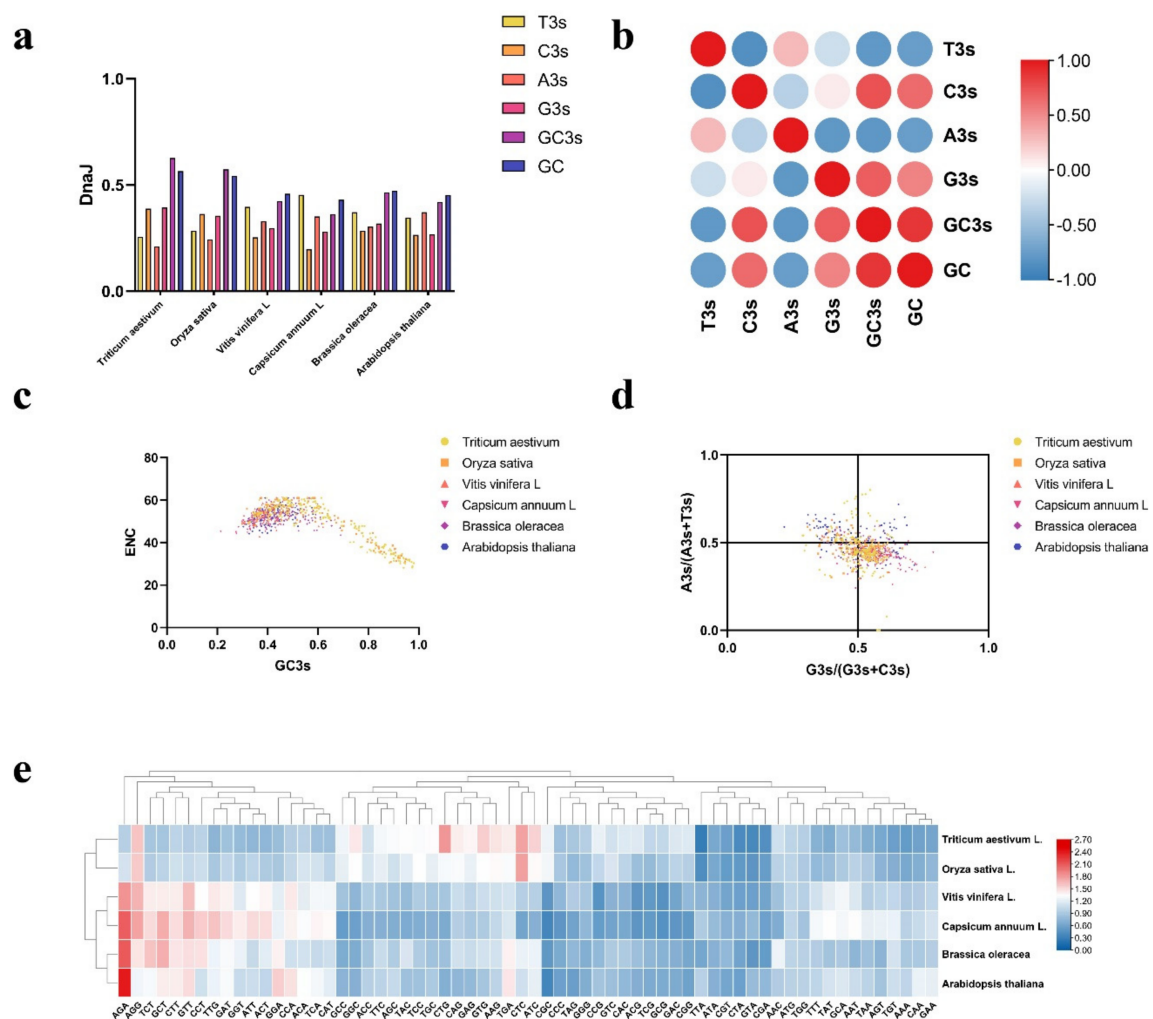


Figure 7. Codon usage pattern analysis of the *DnaJ* gene family in six species. (a) The different colored bars represent the third base frequency. (b) The red and blue colors represent the correlation coefficients of the third base frequency in *Vitis vinifera* L. (c) The different colored and shaped points represent a single gene in each species. (d) The AT bias ($A3s/A3s+T3s$) as the ordinate and the GC bias ($G3s/G3s+C3s$) as the abscissa. (e) The color from blue to red indicates low to high RSCU value of each codon in six species.

2.6. Tissue-Specific Analysis of *VvDnaJs*

To validate the expression patterns of *VvDnaJs*, eight tissues were sampled from grape mature plants, and used for qRT-PCR analysis to determine the expression levels of 12 *VvDnaJs* in ‘YinHong’ grape (Figure 8). We found that the expression levels in stem were relatively lower in 11 *VvDnaJs*. Additionally, most *VvDnaJs* had relatively higher expression levels in fruit skin. VIT_00s0324g00040, VIT_10s0003g00260, VIT_06s0080g01230, and VIT_05s0077g02380 showed the highest expression levels in seed, suggesting that these genes may be involved in seed germination or dormancy. In addition, VIT_06s0080g01230, VIT_17s0000g05530, VIT_07s0005g01220, VIT_01s0010g03760, VIT_03s0038g04420, and VIT_05s0077g02380 had the lowest expression levels in flesh. The expression patterns of *VvDnaJs* within same group showed significant differences, indicating that *VvDnaJs* play different role in different tissues during plant growth and development.

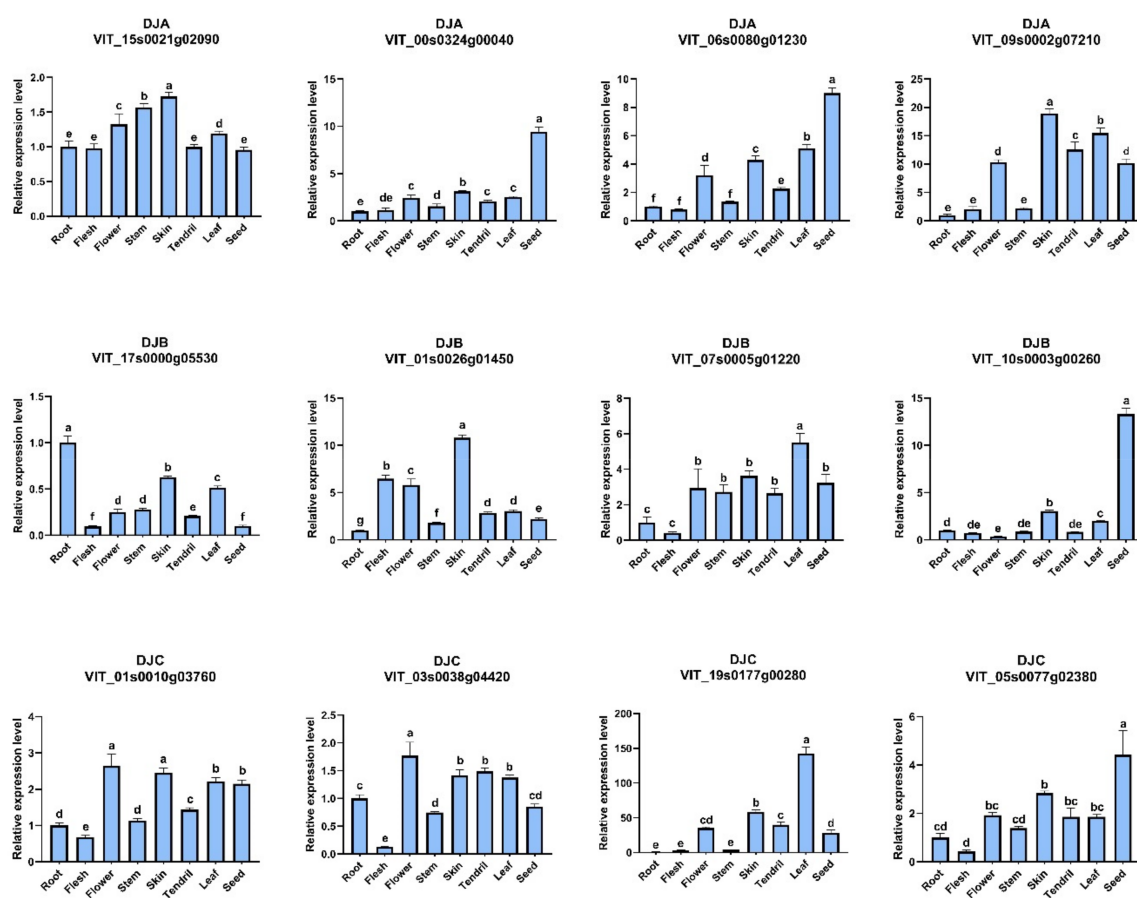


Figure 8. Tissue-specific analysis of 12 *VvDnaJs* based on qRT-PCR. The relative expression levels of 12 selected *VvDnaJs* were determined by qRT-PCR and visualized as histograms. Three biological replicates were sampled for RNA extraction and qRT-PCR analysis when grape plants reached the age of 2 months. Error bars represent the SD ($n = 3$), and a, b, c, . . . above the bars represent a significant difference ($p < 0.05$).

2.7. Prediction of *VvDnaJs* Cis-Acting Elements

To better understand the functions and mechanisms of *VvDnaJs* in transcriptional regulation, the *cis*-acting elements were identified within a 2000 bp upstream region using the PlantCARE database. The identified *cis*-acting regulatory elements can be classified into four functional groups—namely, the binding site, light, hormone, and promoter (Figure S6). A total of 813 *cis*-acting elements related to light responsiveness among *VvDnaJs* were identified, which indicated that the *VvDnaJ* gene family may be involved in light responsiveness. The *cis*-acting elements could be identified in all *VvDnaJs* except for VIT_08s0007g09040, VIT_05s0077g02380, and VIT_08s0032g00960. The *cis*-acting elements are mainly dominated by the binding site. Notably, almost all *VvDnaJs* contain the hormone responsiveness elements, the regulatory elements of hormones such as methyl jasmonate (MeJA), abscisic acid (ABA), gibberellin (GA), salicylic acid (SA), and auxin (Figure 9a), indicating that the *VvDnaJ* gene family could be significantly affected by hormones. Additionally, we found that the CGTCA-motif and TGACG-motif were involved in MeJA responsiveness; ABER in the abscisic acid responsiveness; while P-box, TATC-box and GARE-motif were involved in gibberellin responsiveness; TCA in salicylic acid responsiveness; TGA-box and AuxRR in auxin responsiveness (Table S5). In addition, most *VvDnaJs* contained the enhancer-like elements which were related to anaerobic and anoxic specific induction (Figure 9b).

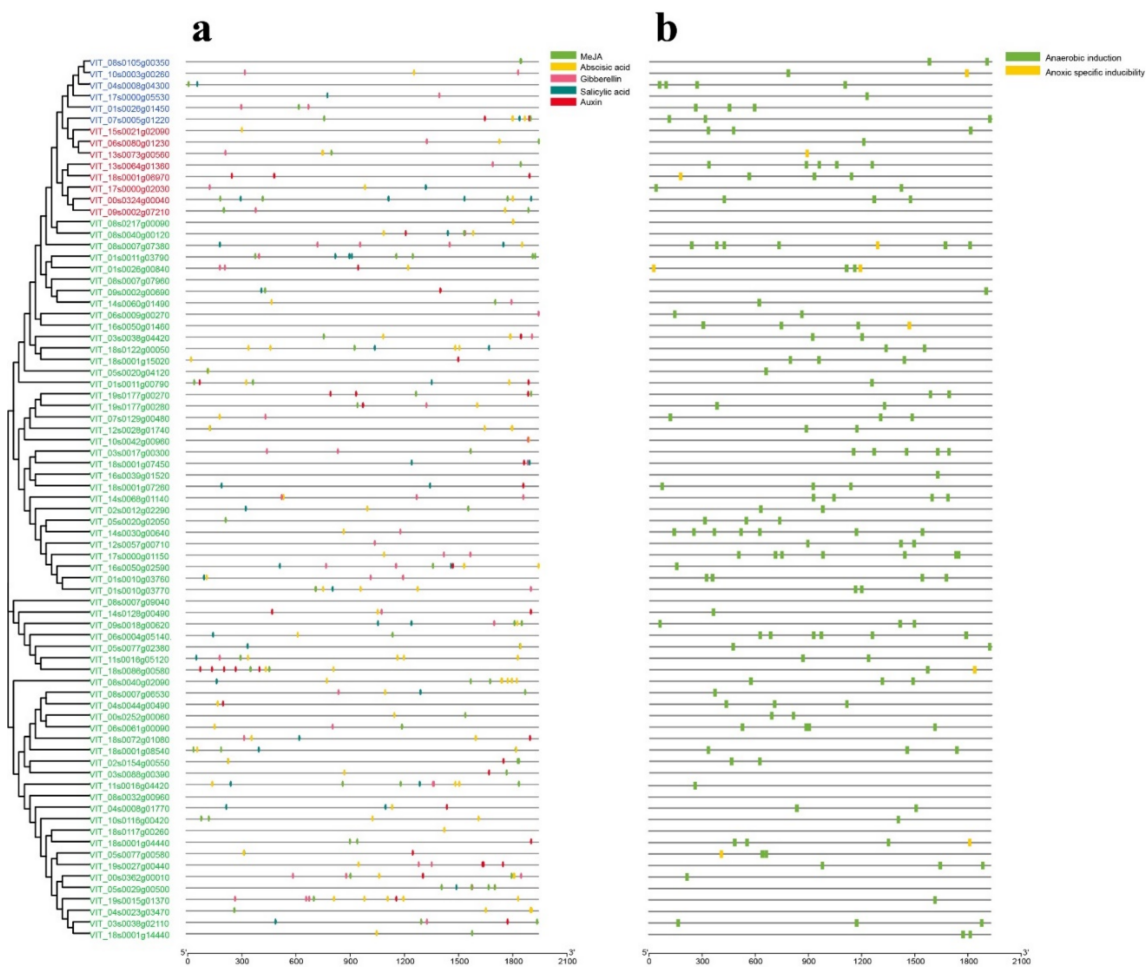


Figure 9. Cis-acting regulatory element analysis of *VvDnaJ* gene family. (a) The type, number and location of hormone-related elements were displayed in different colored dots. (b) The green and yellow dots represent anaerobic induction and anoxic specific induction, respectively.

2.8. Analysis of *VvDnaJ* Expression under Hormone, Shade, Salt, and Heat Stress

It has been established that phytohormones (plant hormones) play a central role in plant physiological processes, which act as a chemical signal molecule and can modify endogenous programs to respond to exogenous signals [31,32]. Additionally, phytohormones are also involved in the physiological responses to biotic and abiotic stresses [33]. Since nearly all *VvDnaJs* contain hormone responsiveness elements. To explore the regulatory mechanisms of the *VvDnaJ* gene family under hormone treatment, two *VvDnaJs* were selected from DJA, DJB, and DJC groups respectively with hormone treatment (SA and MeJA) and determined the expression levels by qRT-PCR. Under hormone treatment (Figure 10a,b), the expression level of VIT_00s0324g00040 reached its peak at 4 h in MeJA treatment, indicating its expressional regulation by MeJA. Compared to other *VvDnaJs*, the VIT_03s0038g04420 was less sensitive to SA treatment. Notably, the expression levels of six *VvDnaJs* were all markedly increased at 5 min under hormone treatment, especially VIT_01s0010g03760.

showed a significant increase under different shading rates compared with the control. This is particularly obvious in the case of the VIT_00s0324g00040 (DJA) when the shading rate was 70%. The VIT_15s0021g02090 (DJA) presented high expression in all treatment groups, which suggested that the members of the DJA group might play an essential regulatory role in shade stress. Salt stress usually occurs as mixed salt stress with both neutral and alkaline salts in nature [36]. However, due to limitations in materials, sodium chloride solution was selected for salt stress treatment. Under salt stress (Figure 10d), the expression levels of VIT_00s0324g00040, VIT_17s0000g05530, VIT_01s0026g01450, and VIT_03s0038g04420 were inhibited substantially in each salt treatment grape. However, there was not significantly different in the expression of VIT_01s0010g03760 between all treatment groups compared with the control. Under heat stress (Figure 11), 10 *VvDnaJs* showed an obvious increase in 6 h compared to 0 h. VIT_07s0005g01220 and VIT_10s0003g00260 showed a high expression level compared to other *VvDnaJs*, which probably play important roles in responding to heat stress.

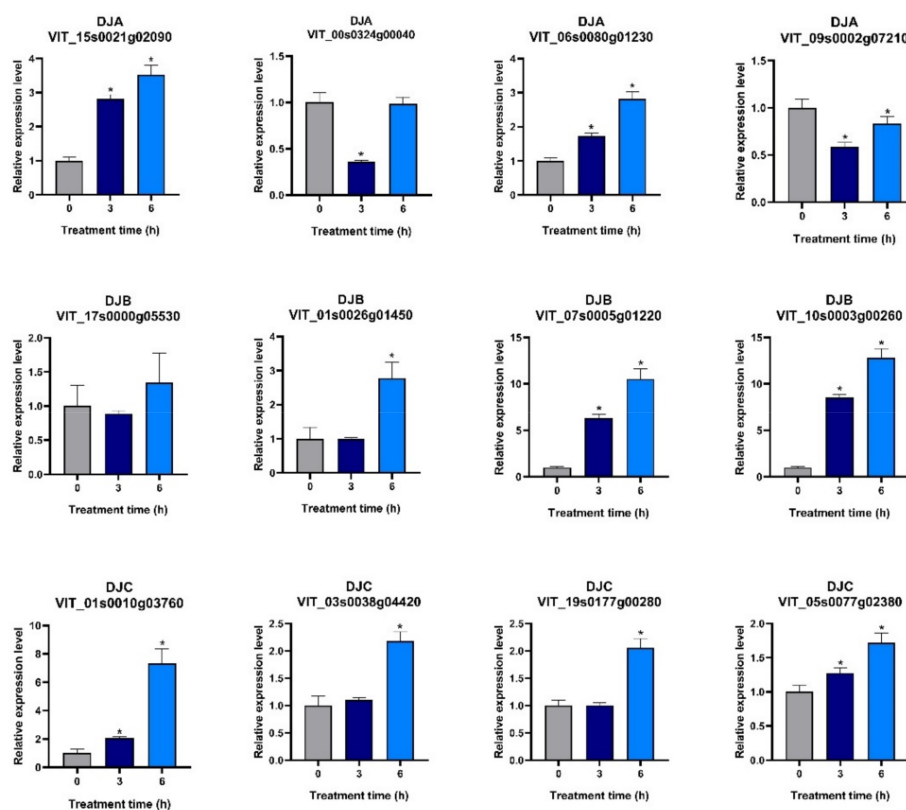


Figure 11. Relative expression levels of 12 *VvDnaJs* in grape plant leaves under heat stress. Three biological replicates were sampled from each treatment for RNA extraction and qRT-PCR analysis. Error bars represent the SD ($n = 3$), and an asterisk (*) above the bars represents a significant difference ($p < 0.05$).

VvDnaJs showed distinct expression patterns among different treatments. For instance, VIT_03s0038g04420 was not sensitive to SA and MeJA treatment, but its expression levels were upregulated under shade, heat stress, and downregulated under salt stress. However, some *VvDnaJs* could respond exceptionally to all five treatments, such as VIT_00s0324g00040. The family genes with different stress responses may form heterodimers with specific proteins, resulting in diverse expression patterns and stress responses [37].

3. Discussion

The DnaJ proteins in an organism are referred to as cellular stress sensors, and are involved in cellular protein homeostasis and tolerance to multiple stresses in plants [38]. Up to now, 76 *DnaJ* genes have been identified in pepper [39], 113 in *Sorghum bicolor* [40], 115 in rice [41], and 117 in *Arabidopsis* [42]. However, little is known about the *DnaJ* gene family in grape. Grape, as a widely recognized fruit, frequently suffers from various environmental stresses in the cultivation process, which lead to substantial yield loss. To investigate the involvement of *VvDnaJs* in responses to these stresses is of great significance for developing cultivation techniques to amelioration of such suffers. In this paper, we identified 78 *VvDnaJs* (Figure 4), which are randomly distributed on 20 chromosomes (Figure S4). The prediction of the protein location showed that the majority of *VvDnaJ* proteins was localized in extracellular matrix (Table 1), indicating that they may be secretory proteins that are associated with cell wall degradation. In the wheat genome, the *DnaJ* gene family was also primarily localized in the extracellular matrix [43]. To verify the accuracy of the prediction results, the recombinant plasmids of VIT_06s0080g01230, VIT_01s0026g01450, VIT_05s0077g02380, VIT_11s0016g05120, VIT_18s0086g00580, and VIT_00s0362g00010 were constructed based on the gateway cloning technique. Except for VIT_01s0026g01450, the subcellular localization results were all consistent with the prediction results (Figure 1). This indicated that each *VvDnaJ* protein played various roles in different organelles.

Exon–intron structural diversity is an important reference for the evolutionary and functional analysis of multiple gene families [44]. 8.97% of *VvDnaJs* has no intron, which is much lower than in rice (20.00%) [41] and *A. thaliana* (22.22%) [42]. In previous studies, genes with few or no introns can be activated or rapidly respond to various stresses [45]. The intron-less gene VIT_01s0010g03760 was a good example that its expression increased rapidly in 5 min after SA and MeJA treatment (Figure 10a,b). In this study, a total of nine motifs were found in the *VvDnaJ* gene family (Figure 5a). All *VvDnaJ* proteins contained motifs 1–3, and the J-domain was composed of motifs 1–3, which is the most conserved among *VvDnaJ* gene family. Additionally, we found that *VvDnaJ* proteins of the same group exhibited similar motif distribution patterns. This was also consistent with a previous study about this gene family.

Gene duplication events are described usually by three elementary gene expansion patterns: tandem duplication, segment duplication, and transposition events. Gene duplication is of great important in genomic rearrangement and the invention of new gene function [46–48]. Six pairs of genes evolved from segmental duplication, and two pairs of genes involved in tandem duplication in our study (Table 2), the total segmental and tandem duplication ratio (16.67%) is much lower than the grape whole-genome duplication ratio, indicating that the segmental and tandem duplication may not be the dominant way of gene expansion in the *VvDnaJ* gene family. The duplication events were mainly observed at Chr3 and Chr18, and these chromosomes may be more active during the process of grape genome evolution (Figure 6).

In different species, codon usage bias (CUB) is the preference of synonymous codon usage in encoding an amino acid, which is widespread in genetics, molecular biology, and gene regulation [49–51]. To determine the codon usage pattern of the *DnaJ* gene in plants, the codon usage percentage, effective number of codon (ENC), parity rule 2 (PR2), and relative synonymous codon usage (RSCU) of the *DnaJ* gene family were calculated in six different species. We found that the codon usage pattern of the *DnaJ* gene family in grape had obvious differences compared to the monocotyledon. In monocotyledon, the usage percentage of C3s and G3s was much higher than that of A3s and T3s (Figure 7a), and the ENC values of some *DnaJ* genes were approximately 20–40 (Figure 7c). In addition, the monocotyledon *DnaJ* genes showed no preference for AGA, while the opposite behavior was observed in dicotyledon (Figure 7e).

Phytohormones play critical roles in helping plants to adapt to various adverse environmental conditions, such as drought, heat, cold, shade, and salinity [52]. SA and

MeJA as the important signal molecules, which are involved in many physiological and biochemical functions and modulate plant responses to stress [53,54]. SA can trigger the expression of *LeCDJ2*, and the expression levels of *LeCDJ2* significantly increased after 3 h under SA treatment [12]. In pepper, the eight *CaDnaJ* genes were clearly induced by MeJA and SA treatment [39]. These findings indicated that *DnaJ* genes were greatly regulated by diverse plant hormones. In our study, we found that the expression of *VvDnaJs* were markedly increased in 5 min under hormone treatment (Figure 10a,b). Some researchers found that application of SA and MeJA to grape leaf can relieve the effects of salt stress [55]. In addition to grape, the application of SA in tomato can restore photosynthetic rates and photosynthetic pigment levels under salt (NaCl) exposure, and numerous physiological indexes were also ameliorated [56]. MeJA can promote growth of salt-stressed *G. uralensis* seedlings by alleviating oxidative stress and strengthening C and N metabolism [57]. In this study, grape plants were subjected to various concentrations of salt stress, and the expression levels of each *VvDnaJ* presented a significant change, this may be also mediated by phytohormone regulation. For example, VIT_17s0000g05530 showed low expression in MeJA and SA treatment, and its expression level was downregulated under salt stress (Figure 10d), which indicated that the downregulation of the affected gene may result from the phytohormone regulation.

Plants are often exposed to high temperatures, the most detrimental factor for crop production [58]. The molecular mechanisms of *DnaJ* proteins involved in heat stress was well investigated. *GmDNJ1* through the surveillance of misfolded proteins for refolding to maintain the full capacity of cellular functions [59]. The expression of *MsDJLP* was rapidly increased in chilling (4 °C) or in heat (42 °C), and the transgenic temperature resistance plants showed to have better relative chlorophyll compositions, water contents, and lower malondialdehyde accumulation than WT plants [60]. In our study, similar results were observed, the expression of 12 *VvDnaJs* under heat stress (35 °C) was significantly increased in 6 h after the treatment, though the degree of the induction was various individually for each *VvDnaJ* (Figure 11). The heat shock transcriptional factor (HSF), one of the most important transcriptional factors of the heat response in sensing and signaling [61], can regulate the expression of the heat shock proteins (HSPs). Therefore, the transcription of *VvDnaJs* may be controlled by HSFs, its upstream regulating genes, for which further investigation is required.

4. Materials and Methods

4.1. Identification of the *DnaJ* Family in *Vitis vinifera* L.

The members of the *DnaJ* family were identified by two steps. Firstly, the hidden Markov model (HMM) profiles of *DnaJ* conserved domain (PF00226), *DnaJ* central domain (PF00648), and *DnaJ* C terminal domain (PF01556) were downloaded in the Pfam database (<http://pfam.xfam.org/>; accessed on 19 May 2021) and used to screen the grape genome to obtain exclusively the *DnaJ* proteins. Then, we used the known *DnaJ* sequences in *Arabidopsis* and rice to blast in the grape genome via a BLASTp search and set an E value threshold (Eval < 10⁻⁶ and ID% > 70) to screen the grape homologs. All results were further screened by the Pfam and SMART databases (<http://smart.embl.de/>; accessed on 20 May 2021) and NCBI-CDD (<https://www.ncbi.nlm.nih.gov/cdd/>; accessed on 20 May 2021). The pep sequences of *VvDnaJ* proteins were extracted from the proteome of grape, and the proteome file was downloaded in Ensembl Plants (http://plants.ensembl.org/Vitis_vinifera/Info/Index; accessed on 20 May 2021). ExPASy was used to calculate the theoretical pl and molecular weight of each *DnaJ* family members (<https://web.expasy.org/protparam/>; accessed on 7 July 2021). SoftBerry was used to predict the protein subcellular localization (<http://linux.softberry.com/>; accessed on 7 July 2021), and the signal peptides for each *VvDnaJ* protein were predicted using SignalP-5.0 (<https://services.healthtech.dtu.dk/service.php?SignalP-5.0>; accessed on 7 July 2021). GO analysis was performed by GENE ONTOLOGY (<http://geneontology.org/>; accessed on 13 October 2021).

4.2. Chromosomal Localization, Phylogenetic, Collinearity, and Ks Analysis

The chromosomal localization data for the *DnaJ* gene family were retrieved from the genome file, and the map was drawn using MapChart. Multiple sequence alignments were performed with the pep sequence of DnaJs for grape, rice, and *Arabidopsis thaliana* using ClustalW in MEGA 6 [62], and the neighbor-joining method (bootstrap: 1000) was used to construct the phylogenetic tree of DnaJ proteins. The collinearity analysis for *VvDnaJs* was calculated by MCScanX, and the results of segmental duplications were illustrated by Circos. The CDS sequences of duplicated gene pairs were aligned using ClustalW. *Ks* (synonymous substitution rate) and *Ka* (nonsynonymous substitution rate) were calculated based on the alignment result using the *KaKs_calculator* script [63]. The formula for the calculation of the divergence time is $T = Ks/2R$, with the R being the rate of divergence for nuclear genes [64]. The R was assumed to be 1.5×10^{-8} synonymous substitutions per gene per year in dicotyledonous plants [65].

4.3. Gene Structure, Conserved Motif, Protein Tertiary Structure, and Multiple Sequence Alignment Analysis

Each *VvDnaJ* cDNA sequence was aligned with the GFF file in order to obtain the data of exon–intron, CDS, and UTR, and the results were obtained using the GSDS (<http://gsds.gao-lab.org/>; accessed on 23 May 2021) [66]. Conserved motif analysis was performed in MEME (<https://meme-suite.org/meme/>; accessed on 23 May 2021) [67], and the number of motifs was set to 10. All the results of the gene structure and motif analysis were imported into TBtools [68]. The protein tertiary structure predictions were performed in SWISS-MODEL (<https://swissmodel.expasy.org/>; accessed on 25 May 2021) [69]. The best model was selected based on QMEAN and GMQE, the larger the value of GMQE (0 to 1) and QMEAN (−4 to 0), the more accurate and better quality it was. DNAMAN software was used to display three *DnaJ* conserved domains and four conserved motifs.

4.4. Codon Usage Pattern Analysis

To systematically analyze the codon usage pattern of *DnaJ* genes in different species, the coding sequences of *DnaJ* genes in *Triticum aestivum*, *Oryza sativa*, *Vitis vinifera* L., *Capsicum annuum* L., *Brassica oleracea*, and *Arabidopsis thaliana* were used to calculate the third site of the synonymous codon for T, C, A, G, and GC contents (T3s, G3s, A3s, C3s, GC3s, and GC content), effective number of codons (ENC) and relative synonymous codon usage (RSCU) with CodonW v1.4.2. The Pearson correlation coefficient method was used to calculate the correlation between different synonymous codons (T3s, C3s, A3s, G3s, GC3s, and GC) in the SPSS software.

4.5. cis-Acting Regulatory Element Analysis

2000 bp DNA sequences upstream of *VvDnaJs* were extracted from the grape genome database, which were used to predict the *cis*-acting elements in the PlantCARE database (<http://bioinformatics.psb.ugent.be/webtools/plantcare/html/>; accessed on 28 May 2021) [70]. The hormone and oxygen responses were determined from the predicting outcomes, and all results were performed using TBtools.

4.6. Plant Materials and Hormone, Shade, Salt, and Heat Treatments

Various tissues including the tendril, leaf, stem, flower, root, seed, flesh, and skin were harvested from the ‘YinHong’ grape plants grown in a greenhouse at Zhejiang Wanli University. Three biological replicates were sampled when plants reached the age of 2 months. The hormone treatment was setup by spraying the plants with 200 μ M SA, 200 μ M MeJA, and distilled water as the control. Triplicate leaf samples were collected randomly at five time intervals (5 min, 2, 4, 6, and 8 h). The shade stress treatment used 40%, 50%, 70%, and 90% transmittance of the sunshade net to cutoff the full sunlight on the plants, again triplicate leaf samples were collected randomly in 15 days after treatment. The salt stress treatment was established by drip-irrigating the plants with 2 (0.2%), 4 (0.4%),

and $6 \text{ g}\cdot\text{L}^{-1}$ (0.6%) sodium chloride solution and leaf samples were collected randomly in 20 days after treatment. For the heat stress treatment, the plants were exposed to $35 \text{ }^{\circ}\text{C}$ and leaves were sampled at 0, 3, and 6 h after treatments. All the samples were frozen by liquid nitrogen and stored at $-80 \text{ }^{\circ}\text{C}$ until total RNA was extracted. Then, the expression levels of *VvDnaJs* were determined with qRT-PCR.

4.7. RNA Extraction and qRT-PCR Analysis

The total RNA for each leaf sample was extracted using the HipPure Plant RNA Mini Kit (Magen), and first-strand cDNA was synthesized using First-Strand cDNA Synthesis SuperMix (Novoprotein). The expression levels of 12 *VvDnaJs* was determined using SYBR qPCR SuperMix Plus (Novoprotein). The primers were designed using Primer 5 software, and the sequences of each primer are listed in Table S6. The $2^{-\Delta\Delta\text{CT}}$ method was used to calculate the relative expression level of 12 *VvDnaJs*. The significance difference was calculated using SPSS software, and the histogram was drawn using GraphPad Prism8 Software.

4.8. Subcellular Localization of *VvDnaJs*

The Gateway cloning technique was used to construct the recombinant plasmid including VIT_06s0080g01230 (cytoplasm), VIT_01s0026g01450 (cytoplasm), VIT_05s0077g02380 (plasma membrane), VIT_11s0016g05120 (plasma membrane), VIT_18s0086g00580 (plasma membrane), and VIT_00s0362g00010 (chloroplast). The first primer pairs were used to amplify the complete encoding sequence. The PCR products were amplified using the second primer pairs. Then, the third primer pairs attB1 and attB2 were used to amplify the products of the previous step. The sequences of each primer described above are listed in Table S7. The final products were introduced into pDonor207 based on the BP reaction, and the entry vectors were constructed. Finally, the fragments were subsequently transferred from the entry vector to the pGWB406 expression vector via LR reaction [71].

The recombinant plasmids were transferred into *Agrobacterium tumefaciens* GV3101 by electric shock, and agro-infiltration was performed as described in [72]. A positive colony was obtained using $50 \text{ }\mu\text{g}\cdot\text{mL}^{-1}$ spectinomycin, gentamicin, and rifampicin for selection in yeast extract tryptone (YEP) solid medium. The *Agrobacterium* cultures containing recombinant plasmid were activated by *Agrobacterium* infiltration solution (10 mM MgCl_2 , 10 mM MES, 200 mM AS), and then infected into *N. benthamiana* leaves. The RFP-TM23 marker protein was used to locate the plasma membrane [73]. The infiltrated leaves were sampled at 3 days post agro-infiltration, and the localization of each protein was observed under a Leica TCS SP5 confocal laser scanning microscope (Leica Microsystems) [74].

5. Conclusions

In this study, a genome-wide analysis of the grape *DnaJ* gene family was performed, and 78 *VvDnaJs* were identified. Then the chromosomal localization, phylogenetic tree, collinearity, gene structure, conserved motif, protein tertiary structure, multiple sequence comparison, codon usage pattern, and *cis*-acting elements of these genes were further analyzed using a range of bioinformatics approaches to reveal the evolutionary mechanisms and processes for the *VvDnaJ* gene family in grape. In addition, the expression pattern analysis showed that *VvDnaJs* exhibited tissue-specific expression and were sensitive to various hormone treatments and abiotic stresses. In summary, this study provided comprehensive information for further investigation on the genetics and protein functions of the *VvDnaJ* gene family.

Supplementary Materials: The following are available online at <https://www.mdpi.com/article/10.3390/horticulturae7120589/s1>, Figure S1: Number of DJA, DJB, and DJC genes in grape, rice, and *Arabidopsis thaliana*; Figure S2: Conserved motifs analysis in *VvDnaJ* gene family; Figure S3: Multiple sequence comparison in DJA and DJB groups; Figure S4: The chromosomal distribution of *VvDnaJs*; Figure S5: ENC-plot and PR2-plot analysis of *DnaJ* genes in six different species; Figure S6: The number of *cis*-acting elements for *VvDnaJs* in five groups; Table S1: List of *DnaJ* coding sequences from *Arabidopsis thaliana*, *Oryza sativa*, and *Vitis vinifera* L.; Table S2: The sequences of nine conserved motifs; Table S3: Codon usage indicators of *DnaJ* genes; Table S4: The relative synonymous codon usage (RSCU) values of *DnaJ* CDS sequences in six species; Table S5: *Cis*-acting components of *DnaJ* genes in grape; Table S6: The primer sequences for qRT-PCR; Table S7: The primer sequences for expression vector construction.

Author Contributions: T.C. participated in writing the manuscript; Z.C., Y.W. and J.Y. were involved in the experimental design. T.C., T.X., T.Z., T.L. and L.S. were involved in the collection and analysis of data. All authors have read and agreed to the published version of the manuscript.

Funding: This research was funded by the Key Research and Development Program of Zhejiang Province (2021C02053) and 2025 Major Science and Technology Innovation Special Project of Ningbo (2019B10015).

Institutional Review Board Statement: Not applicable.

Informed Consent Statement: Not applicable.

Data Availability Statement: Not applicable.

Conflicts of Interest: The authors declare that they have no conflict of interest.

References

- Duan, S.; Wu, Y.; Fu, R.; Wang, L.; Chen, Y.; Xu, W.; Zhang, C.; Ma, C.; Shi, J.; Wang, S. Comparative Metabolic Profiling of Grape Skin Tissue along Grapevine Berry Developmental Stages Reveals Systematic Influences of Root Restriction on Skin Metabolome. *Int. J. Mol. Sci.* **2019**, *20*, 534. [\[CrossRef\]](#)
- Ramos, M.J.N.; Coito, J.L.; Silva, H.G.; Cunha, J.; Costa, M.M.R.; Rocheta, M. Flower development and sex specification in wild grapevine. *BMC Genom.* **2014**, *15*, 1095. [\[CrossRef\]](#) [\[PubMed\]](#)
- Fu, J.; Luo, Y.; Sun, P.; Gao, J.; Zhao, D.; Yang, P.; Hu, T. Effects of shade stress on turfgrasses morphophysiology and rhizosphere soil bacterial communities. *BMC Plant Biol.* **2020**, *20*, 92. [\[CrossRef\]](#)
- Tanveer, M.; Yousaf, U. Plant single-cell biology and abiotic stress tolerance. In *Plant Life under Changing Environment*; Tripathi, D.K., Pratap Singh, V., Chauhan, D.K., Sharma, S., Prasad, S.M., Dubey, N.K., Ramawat, N., Eds.; Academic Press: Cambridge, MA, USA, 2020; pp. 611–626.
- Zhao, Q.; Zhang, H.; Wang, T.; Chen, S.; Dai, S. Proteomics-based investigation of salt-responsive mechanisms in plant roots. *J. Proteom.* **2013**, *82*, 230–253. [\[CrossRef\]](#)
- De Leo, V.; Musacchio, M.C.; Cappelli, V.; Massaro, M.G.; Morgante, G.; Petraglia, F. Genetic, hormonal and metabolic aspects of PCOS: An update. *Reprod. Biol. Endocrinol.* **2016**, *14*, 38. [\[CrossRef\]](#) [\[PubMed\]](#)
- Park, C.J.; Seo, Y.S. Heat Shock Proteins: A Review of the Molecular Chaperones for Plant Immunity. *Plant Pathol. J.* **2015**, *31*, 323–333. [\[CrossRef\]](#) [\[PubMed\]](#)
- Martine, P.; Rébé, C. Heat Shock Proteins and Inflammasomes. *Int. J. Mol. Sci.* **2019**, *20*, 4508. [\[CrossRef\]](#)
- Wang, G.; Kong, F.; Zhang, S.; Meng, X.; Wang, Y.; Meng, Q. A tomato chloroplast-targeted DnaJ protein protects Rubisco activity under heat stress. *J. Exp. Bot.* **2015**, *66*, 3027–3040. [\[CrossRef\]](#)
- Fan, C.-Y.; Lee, S.; Cyr, D.M. Mechanisms for regulation of Hsp70 function by Hsp40. *Cell Stress Chaperones* **2003**, *8*, 309–316. [\[CrossRef\]](#)
- Caplan, A.J.; Cyr, D.M.; Douglas, M.G. Eukaryotic homologues of Escherichia coli dnaJ: A diverse protein family that functions with hsp70 stress proteins. *Mol. Biol. Cell* **1993**, *4*, 555–563. [\[CrossRef\]](#)
- Wang, G.; Cai, G.; Kong, F.; Deng, Y.; Ma, N.; Meng, Q. Overexpression of tomato chloroplast-targeted DnaJ protein enhances tolerance to drought stress and resistance to *Pseudomonas solanacearum* in transgenic tobacco. *Plant Physiol. Biochem.* **2014**, *82*, 95–104. [\[CrossRef\]](#) [\[PubMed\]](#)
- Rajan, V.B.; D’Silva, P. Arabidopsis thaliana J-class heat shock proteins: Cellular stress sensors. *Funct. Integr. Genom.* **2009**, *9*, 433–446. [\[CrossRef\]](#) [\[PubMed\]](#)
- Pulido, P.; Leister, D. Novel DNAJ-related proteins in Arabidopsis thaliana. *New Phytol.* **2018**, *217*, 480–490. [\[CrossRef\]](#) [\[PubMed\]](#)
- Liu, J.Z.; Whitham, S.A. Overexpression of a soybean nuclear localized type-III DnaJ domain-containing HSP40 reveals its roles in cell death and disease resistance. *Plant J.* **2013**, *74*, 110–121. [\[CrossRef\]](#)

16. Walsh, P.; Bursac, D.; Law, Y.C.; Cyr, D.; Lithgow, T. The J-protein family: Modulating protein assembly, disassembly and translocation. *EMBO Rep.* **2004**, *5*, 567–571. [[CrossRef](#)]
17. Kong, F.; Deng, Y.; Wang, G.; Wang, J.; Liang, X.; Meng, Q. LeCDJ1, a chloroplast DnaJ protein, facilitates heat tolerance in transgenic tomatoes. *J. Integr. Plant Biol.* **2014**, *56*, 63–74. [[CrossRef](#)]
18. Bekh-Ochir, D.; Shimada, S.; Yamagami, A.; Kanda, S.; Ogawa, K.; Nakazawa, M.; Matsui, M.; Sakuta, M.; Osada, H.; Asami, T.; et al. A novel mitochondrial DnaJ/Hsp40 family protein BIL2 promotes plant growth and resistance against environmental stress in brassinosteroid signaling. *Planta* **2013**, *237*, 1509–1525. [[CrossRef](#)] [[PubMed](#)]
19. Hofius, D.; Maier, A.T.; Dietrich, C.; Jungkunz, I.; Börnke, F.; Maiss, E.; Sonnewald, U. Capsid protein-mediated recruitment of host DnaJ-like proteins is required for Potato virus Y infection in tobacco plants. *J. Virol.* **2007**, *81*, 11870–11880. [[CrossRef](#)]
20. Tamadaddi, C.; Sagar, V.; Verma, A.K.; Afsal, F.; Sahi, C. Expansion of the evolutionarily conserved network of J-domain proteins in the Arabidopsis mitochondrial import complex. *Plant Mol. Biol.* **2021**, *105*, 385–403. [[CrossRef](#)]
21. Park, M.; Kim, S. The Arabidopsis J Protein AtJ1 is Essential for Seedling Growth, Flowering Time Control and ABA Response. *Plant Cell Physiol.* **2014**, *55*, 2152–2163. [[CrossRef](#)]
22. Verma, A.K.; Tamadaddi, C.; Tak, Y.; Lal, S.S.; Cole, S.J.; Hines, J.K.; Sahi, C. The expanding world of plant J-domain proteins. *Crit. Rev. Plant Sci.* **2019**, *38*, 382–400. [[CrossRef](#)]
23. Yu, X.; Mo, Z.; Tang, X.; Gao, T.; Mao, Y. Genome-wide analysis of HSP70 gene superfamily in *Pyropia yezoensis* (Bangiales, Rhodophyta): Identification, characterization and expression profiles in response to dehydration stress. *BMC Plant Biol.* **2021**, *21*, 435. [[CrossRef](#)] [[PubMed](#)]
24. Müller, A.; Rinck, G.; Thiel, H.J.; Tautz, N. Cell-derived sequences in the N-terminal region of the polyprotein of a cytopathogenic pestivirus. *J. Virol.* **2003**, *77*, 10663–10669. [[CrossRef](#)] [[PubMed](#)]
25. Ajit Tamadaddi, C.; Sahi, C. J domain independent functions of J proteins. *Cell Stress Chaperones* **2016**, *21*, 563–570. [[CrossRef](#)] [[PubMed](#)]
26. Jeffreys, A.J.; Harris, S. Processes of gene duplication. *Nature* **1982**, *296*, 9–10. [[CrossRef](#)]
27. Liu, Y.; Wang, Y.; Pei, J.; Li, Y.; Sun, H. Genome-wide identification and characterization of COMT gene family during the development of blueberry fruit. *BMC Plant Biol.* **2021**, *21*, 5. [[CrossRef](#)]
28. Uddin, D.A. Codon Usage Bias: A Tool for Understanding Molecular Evolution. *J. Proteom. Bioinform.* **2017**, *10*, e32. [[CrossRef](#)]
29. Wu, H.; Bao, Z.; Mou, C.; Chen, Z.; Zhao, J. Comprehensive Analysis of Codon Usage on Porcine Astrovirus. *Viruses* **2020**, *12*, 991. [[CrossRef](#)]
30. Hu, L.; Wang, P.; Hao, Z.; Lu, Y.; Xue, G.; Cao, Z.; Qu, H.; Cheng, T.; Shi, J.; Chen, J. Gibberellin Oxidase Gene Family in *L. chinense*: Genome-Wide Identification and Gene Expression Analysis. *Int. J. Mol. Sci.* **2021**, *22*, 7167. [[CrossRef](#)]
31. Gräfe, K.; Shanmugarajah, K.; Zobel, T.; Weidtkamp-Peters, S.; Kleinschrodt, D.; Smits, S.H.J.; Schmitt, L. Cloning and expression of selected ABC transporters from the Arabidopsis thaliana ABCG family in *Pichia pastoris*. *PLoS ONE* **2019**, *14*, e0211156. [[CrossRef](#)] [[PubMed](#)]
32. Chung, Y.; Kwon, S.I.; Choe, S. Antagonistic regulation of Arabidopsis growth by brassinosteroids and abiotic stresses. *Mol. Cells* **2014**, *37*, 795–803. [[CrossRef](#)]
33. Müller, M.; Munné-Bosch, S. Hormone Profiling in Plant Tissues. In *Plant Hormones: Methods and Protocols*; Kleine-Vehn, J., Sauer, M., Eds.; Springer: New York, NY, USA, 2017; pp. 249–258.
34. Zhang, Y.; Jiang, L.; Li, Y.; Chen, Q.; Ye, Y.; Zhang, Y.; Luo, Y.; Sun, B.; Wang, X.; Tang, H. Effect of Red and Blue Light on Anthocyanin Accumulation and Differential Gene Expression in Strawberry (*Fragaria × ananassa*). *Molecules* **2018**, *23*, 820. [[CrossRef](#)]
35. Yang, B.; Tang, J.; Yu, Z.; Khare, T.; Srivastav, A.; Datir, S.; Kumar, V. Light Stress Responses and Prospects for Engineering Light Stress Tolerance in Crop Plants. *J. Plant Growth Regul.* **2019**, *38*, 1489–1506. [[CrossRef](#)]
36. Liu, J.; Shen, F.; Xiao, Y.; Fang, H.; Qiu, C.; Li, W.; Wu, T.; Xu, X.; Wang, Y.; Zhang, X.; et al. Genomics-assisted prediction of salt and alkali tolerances and functional marker development in apple rootstocks. *BMC Genom.* **2020**, *21*, 550. [[CrossRef](#)] [[PubMed](#)]
37. Wang, R.; Zhao, P.; Kong, N.; Lu, R.; Pei, Y.; Huang, C.; Ma, H.; Chen, Q. Genome-Wide Identification and Characterization of the Potato bHLH Transcription Factor Family. *Genes* **2018**, *9*, 54. [[CrossRef](#)] [[PubMed](#)]
38. Deng, Y.; Hu, Z.; Shang, L.; Chai, Z.; Tang, Y.Z. Transcriptional Responses of the Heat Shock Protein 20 (Hsp20) and 40 (Hsp40) Genes to Temperature Stress and Alteration of Life Cycle Stages in the Harmful Alga *Scrippsiella trochoidea* (Dinophyceae). *Biology* **2020**, *9*, 408. [[CrossRef](#)] [[PubMed](#)]
39. Fan, F.F.; Liu, F.; Yang, X.; Wan, H.; Kang, Y. Global analysis of expression profile of members of DnaJ gene families involved in capsaicinoids synthesis in pepper (*Capsicum annuum* L.). *BMC Plant Biol.* **2020**, *20*, 326. [[CrossRef](#)]
40. Nagaraju, M.; Kumar, A.; Rajasheker, G.; Manohar Rao, D.; Kavi Kishor, P.B. DnaJs, the critical drivers of Hsp70s: Genome-wide screening, characterization and expression of DnaJ family genes in *Sorghum bicolor*. *Mol. Biol. Rep.* **2020**, *47*, 7379–7390. [[CrossRef](#)] [[PubMed](#)]
41. Luo, Y.; Fang, B.; Wang, W.; Yang, Y.; Rao, L.; Zhang, C. Genome-wide analysis of the rice J-protein family: Identification, genomic organization, and expression profiles under multiple stresses. *3 Biotech* **2019**, *9*, 358. [[CrossRef](#)]
42. Zhang, B.; Qiu, H.-L.; Qu, D.-H.; Ruan, Y.; Chen, D.-H. Phylogeny-dominant classification of J-proteins in Arabidopsis thaliana and Brassica oleracea. *Genome* **2018**, *61*, 405–415. [[CrossRef](#)] [[PubMed](#)]

43. Zhang, R.; Liu, C.; Song, X.; Sun, F.; Xiao, D.; Wei, Y.; Hou, X.; Zhang, C. Genome-wide identification and analysis of the regulation wheat DnaJ family genes following wheat yellow mosaic virus infection. *3 Biotech* **2020**, *10*, 363. [[CrossRef](#)]
44. Yan, J.; Ma, Z.; Xu, X.; Guo, A.-Y. Evolution, functional divergence and conserved exon–intron structure of bHLH/PAS gene family. *Mol. Genet. Genom.* **2014**, *289*, 25–36. [[CrossRef](#)]
45. Jeffares, D.C.; Penkett, C.J.; Bähler, J. Rapidly regulated genes are intron poor. *Trends Genet. TIG* **2008**, *24*, 375–378. [[CrossRef](#)]
46. Cheng, C.; Wang, Y.; Chai, F.; Li, S.; Xin, H.; Liang, Z. Genome-wide identification and characterization of the 14–3–3 family in *Vitis vinifera* L. during berry development and cold and heat-stress response. *BMC Genom.* **2018**, *19*, 579. [[CrossRef](#)]
47. He, J.; Zhao, H.; Cheng, Z.; Ke, Y.; Liu, J.; Ma, H. Evolution Analysis of the Fasciclin-Like Arabinogalactan Proteins in Plants Shows Variable Fasciclin-AGP Domain Constitutions. *Int. J. Mol. Sci.* **2019**, *20*, 1945. [[CrossRef](#)] [[PubMed](#)]
48. Lopez-Ortiz, C.; Peña-García, Y.; Natarajan, P.; Bhandari, M.; Abburi, V.; Dutta, S.K.; Yadav, L.; Stommel, J.; Nimmakayala, P.; Reddy, U.K. The ankyrin repeat gene family in *Capsicum* spp: Genome-wide survey, characterization and gene expression profile. *Sci. Rep.* **2020**, *10*, 4044. [[CrossRef](#)] [[PubMed](#)]
49. Chakraborty, S.; Deb, B.; Barbhuiya, P.A.; Uddin, A. Analysis of codon usage patterns and influencing factors in Nipah virus. *Virus. Res.* **2019**, *263*, 129–138. [[CrossRef](#)]
50. Carlini, D.B.; Stephan, W. In vivo introduction of unpreferred synonymous codons into the *Drosophila Adh* gene results in reduced levels of ADH protein. *Genetics* **2003**, *163*, 239–243. [[CrossRef](#)]
51. Roberts, R.J. Restriction and modification enzymes and their recognition sequences. *Nucleic Acids Res.* **1981**, *9*, 213. [[CrossRef](#)] [[PubMed](#)]
52. Verma, V.; Ravindran, P.; Kumar, P. Plant hormone-mediated regulation of stress responses. *BMC Plant Biol.* **2016**, *16*, 1–10. [[CrossRef](#)]
53. Arfan, M.; Athar, H.R.; Ashraf, M. Does exogenous application of salicylic acid through the rooting medium modulate growth and photosynthetic capacity in two differently adapted spring wheat cultivars under salt stress? *J. Plant Physiol.* **2007**, *164*, 685–694. [[CrossRef](#)]
54. Yu, X.; Zhang, W.; Zhang, Y.; Zhang, X.; Lang, D.; Zhang, X. The roles of methyl jasmonate to stress in plants. *Funct. Plant Biol.* **2019**, *46*, 197–212. [[CrossRef](#)]
55. Odabaşoğlu, M.; Demirtaş, G.; Yildirim, K.; Gürsöz, S. Salt Stress on Grapes (*Vitis* spp). In Proceedings of the International Gap Agriculture & Livestock Congress, Şanlıurfa, Turkey, 25–27 April 2018.
56. Mimouni, H.; Wasti, S.; Manaa, A.; Gharbi, E.; Chalh, D.A.; Vandoorne, B.; Ben Ahmed, H. Does Salicylic Acid (SA) Improve Tolerance to Salt Stress in Plants? A Study of SA Effects On Tomato Plant Growth, Water Dynamics, Photosynthesis, and Biochemical Parameters. *OMICS A J. Integr. Biol.* **2016**, *20*, 180–190. [[CrossRef](#)]
57. Lang, D.; Yu, X.; Jia, X.; Li, Z.; Zhang, X. Methyl jasmonate improves metabolism and growth of NaCl-stressed *Glycyrrhiza uralensis* seedlings. *Sci. Hort.* **2020**, *266*, 109287. [[CrossRef](#)]
58. Hatfield, J.L.; Prueger, J.H. Temperature extremes: Effect on plant growth and development. *Weather. Clim. Extrem.* **2015**, *10*, 4–10. [[CrossRef](#)]
59. Li, K.-P.; Wong, C.-H.; Cheng, C.-C.; Cheng, S.-S.; Li, M.-W.; Mansveld, S.; Bergsma, A.; Huang, T.; Van Eijk, M.J.T.; Lam, H.-M. GmDNJ1, a type-I heat shock protein 40 (HSP40), is responsible for both Growth and heat tolerance in soybean. *Plant Direct* **2021**, *5*, e00298. [[CrossRef](#)] [[PubMed](#)]
60. Lee, K.W.; Rahman, M.A.; Kim, K.Y.; Choi, G.J.; Cha, J.Y.; Cheong, M.S.; Shohael, A.M.; Jones, C.; Lee, S.H. Overexpression of the alfalfa DnaJ-like protein (MsDJLP) gene enhances tolerance to chilling and heat stresses in transgenic tobacco plants. *Turk. J. Biol.* **2018**, *42*, 12–22. [[CrossRef](#)] [[PubMed](#)]
61. Liu, G.; Chai, F.; Wang, Y.; Jiang, J.; Duan, W.; Wang, Y.; Wang, F.; Li, S.; Wang, L. Genome-wide Identification and Classification of HSF Family in Grape, and Their Transcriptional Analysis under Heat Acclimation and Heat Stress. *Hortic. Plant J.* **2018**, *4*, 133–143. [[CrossRef](#)]
62. Tamura, K.; Stecher, G.; Peterson, D.; Filipowski, A.; Kumar, S. MEGA6: Molecular Evolutionary Genetics Analysis version 6.0. *Mol. Biol. Evol.* **2013**, *30*, 2725–2729. [[CrossRef](#)]
63. Zhang, Z.; Li, J.; Zhao, X.-Q.; Wang, J.; Wong, G.K.-S.; Yu, J. KaKs_Calculator: Calculating Ka and Ks Through Model Selection and Model Averaging. *Genom. Proteom. Bioinform.* **2006**, *4*, 259–263. [[CrossRef](#)]
64. Huang, Z.; Duan, W.; Song, X.; Tang, J.; Wu, P.; Zhang, B.; Hou, X. Retention, Molecular Evolution, and Expression Divergence of the Auxin/Indole Acetic Acid and Auxin Response Factor Gene Families in Brassica Rapa Shed Light on Their Evolution Patterns in Plants. *Genome Biol. Evol.* **2016**, *8*, 302–316. [[CrossRef](#)] [[PubMed](#)]
65. Koch, M.A.; Haubold, B.; Mitchell-Olds, T. Comparative Evolutionary Analysis of Chalcone Synthase and Alcohol Dehydrogenase Loci in Arabidopsis, Arabis, and Related Genera (Brassicaceae). *Mol. Biol. Evol.* **2000**, *17*, 1483–1498. [[CrossRef](#)] [[PubMed](#)]
66. Hu, B.; Jin, J.; Guo, A.Y.; Zhang, H.; Luo, J.; Gao, G. GSDS 2.0: An upgraded gene feature visualization server. *Bioinformatics* **2015**, *31*, 1296–1297. [[CrossRef](#)] [[PubMed](#)]
67. Bailey, T.L.; Boden, M.; Buske, F.A.; Frith, M.; Grant, C.E.; Clementi, L.; Ren, J.; Li, W.W.; Noble, W.S. MEME SUITE: Tools for motif discovery and searching. *Nucleic Acids Res.* **2009**, *37*, W202–W208. [[CrossRef](#)]
68. Chen, C.; Chen, H.; Zhang, Y.; Thomas, H.R.; Frank, M.H.; He, Y.; Xia, R. TBtools: An Integrative Toolkit Developed for Interactive Analyses of Big Biological Data. *Mol. Plant* **2020**, *13*, 1194–1202. [[CrossRef](#)]

69. Berman, H.M.; Westbrook, J.; Feng, Z.; Gilliland, G.; Bhat, T.N.; Weissig, H.; Shindyalov, I.N.; Bourne, P.E. The Protein Data Bank. *Nucleic Acids Res.* **2000**, *28*, 235–242. [[CrossRef](#)]
70. Lescot, M.; Déhais, P.; Thijs, G.; Marchal, K.; Moreau, Y.; Van de Peer, Y.; Rouzé, P.; Rombauts, S. PlantCARE, a database of plant cis-acting regulatory elements and a portal to tools for in silico analysis of promoter sequences. *Nucleic Acids Res.* **2002**, *30*, 325–327. [[CrossRef](#)]
71. Zhang, T.; Liu, P.; Zhong, K.; Zhang, F.; Xu, M.; He, L.; Jin, P.; Chen, J.; Yang, J. Wheat Yellow Mosaic Virus NIb Interacting with Host Light Induced Protein (LIP) Facilitates Its Infection through Perturbing the Abscisic Acid Pathway in Wheat. *Biology* **2019**, *8*, 80. [[CrossRef](#)]
72. Wang, A. Dissecting the molecular network of virus-plant interactions: The complex roles of host factors. *Annu. Rev. Phytopathol.* **2015**, *53*, 45–66. [[CrossRef](#)]
73. Bueso, E.; Rodriguez, L.; Lorenzo-Orts, L.; Gonzalez-Guzman, M.; Sayas, E.; Muñoz-Bertomeu, J.; Ibañez, C.; Serrano, R.; Rodriguez, P.L. The single-subunit RING-type E3 ubiquitin ligase RSL1 targets PYL4 and PYR1 ABA receptors in plasma membrane to modulate abscisic acid signaling. *Plant J.* **2014**, *80*, 1057–1071. [[CrossRef](#)]
74. He, L.; Chen, X.; Yang, J.; Zhang, T.; Li, J.; Zhang, S.; Zhong, K.; Zhang, H.; Chen, J.; Yang, J. Rice black-streaked dwarf virus-encoded P5-1 regulates the ubiquitination activity of SCF E3 ligases and inhibits jasmonate signaling to benefit its infection in rice. *New Phytol.* **2020**, *225*, 896–912. [[CrossRef](#)] [[PubMed](#)]